Head Removal Enhances Planarian Electrotaxis

Ziad Sabry[1], Rui Wang[1,2], Aryo Jahromi[3], Christina Rabeler[1], William B. Kristan[4], Eva-Maria S. Collins[1,5,6,*]

[1]Department of Biology, Swarthmore College, Swarthmore, Pennsylvania, USA

[2]Department of Bioengineering, University of California San Diego, La Jolla, California, USA

[3]Department of Mechanical Engineering, University of California San Diego, La Jolla, California, USA

[4]Department of Biological Sciences, California State University San Marcos, San Marcos, California, USA

[5]Department of Physics and Astronomy, Swarthmore College, Swarthmore, Pennsylvania, USA

[6]Department of Physics, University of California San Diego, La Jolla, California, USA

[*]Author for correspondence: ecollin3@swarthmore.edu

Keywords: planarian, electrotaxis, galvanotaxis, locomotion, decapitation

Summary statement: We present a new method for quantitative studies of planarian electrotaxis and show that *Dugesia japonica* move toward the cathode. This behavior is enhanced by removal of the head.

Abstract

Certain animal species utilize electric fields for communication, hunting, and spatial orientation. Freshwater planarians move toward the cathode in a static electric field (cathodic electrotaxis). This planarian behavior was first described by Raymond Pearl more than a century ago. However, planarian electrotaxis has received little attention since, and the underlying

mechanisms and evolutionary significance remain unknown. To close this knowledge gap, we developed an apparatus and scoring metrics for automated quantitative and mechanistic studies of planarian behavior upon exposure to a static electric field. Using this automated setup, we characterized electrotaxis in the planarian *Dugesia japonica* and found that this species responds to voltage instead of to current, in contrast to results from previous studies using other planarian species. Surprisingly, we found differences in electrotaxis ability between small (shorter) and large (longer) planarians. To determine the cause of these differences, we took advantage of the regenerative abilities of planarians and compared electrotaxis in head, tail, and trunk fragments of various lengths. We found that tail and trunk fragments electrotaxed while head fragments did not, regardless of size. Based on these data, we hypothesized that signals from the head may interfere with electrotaxis when the head area/body area reached a critical threshold. In support of this hypothesis, we found that (a) smaller intact planarians which cannot electrotax have a relatively larger head-to-body-ratio than large planarians which can electrotax, and that (b) electrotaxis behavior of cut head fragments was negatively correlated with the head-to-body ratio of the fragments. Moreover, we could restore cathodic electrotaxis in head fragments via decapitation, directly demonstrating inhibition of electrotaxis by the head.

Introduction

Freshwater planarians are several mm long soft-bodied flatworms famous for their regenerative abilities (Rink, 2018). Planarians have a large repertoire of behaviors that can be used as readouts of brain function (Inoue *et al.*, 2015; Zhang *et al.*, 2019). Over a century ago, Raymond Pearl (1903) was the first to write a comprehensive description of planarian behaviors, including ciliary driven gliding and musculature driven locomotion (peristalsis, scrunching), phototaxis, chemotaxis, and thermotaxis. Recently, planarians have experienced a resurgence as a neurobiology system because modern molecular biology techniques paired with computer vision now allow for mechanistic and quantitative studies of their behavior. For example, it was shown that ciliary gliding depends on serotonergic signaling (Currie and Pearson, 2013), that peristalsis and scrunching are distinct gaits (Cochet-Escartin, Mickolajczk and Collins, 2015), with peristalsis resulting from non-functional cilia (Rompolas, Patel-King and King, 2010) and scrunching being a cilia-independent escape gait (Cochet-Escartin, Mickolajczk and Collins,

2015). Thermo-, photo-, and chemotaxis have been found to require the presence of a brain to sense their respective stimuli (Inoue *et al.*, 2015), whereas fission (Malinowski *et al.*, 2017; Goel *et al.*, 2021), scrunching (Cochet-Escartin, Mickolajczk and Collins, 2015), and avoidance of local near-UV stimulation (Paskin *et al.*, 2014; Shettigar *et al.*, 2017; Le *et al.*, 2021; Nishan *et al.*, 2021) can occur without a brain.

Here, we characterize electrotaxis, another planarian behavior which was first described by Pearl over a century ago (Pearl, 1903) but, to the best of our knowledge, has not been rigorously revisited. Pearl showed that members of various planarian species **(***Planaria maculata, P. dorotocephala, P. gonocephala;* **Table S1)** turn towards the negatively charged electrode (cathode) when an electrical field is applied (Pearl, 1903). He observed that the end of the planarian closest to the positively charged electrode (anode) contracted, comparable to the response observed by mechanical stimulation. Pearl interpreted this as evidence of the current acting directly on the muscles rather than interacting with sensory organs or cilia. Furthermore, he reported that planarians became "wholly or partially paralyzed in a very short time after the current begins to act, and as a consequence the reactions become feeble and indistinct" (Pearl, 1903). Unfortunately, no information on the duration of these experiments was provided, but this description of the planarians' behavior suggests the use of strong electric fields. Finally, Pearl found that head pieces from transversely cut planarians behaved identically to intact worms while tail pieces displayed contraction on the anode-facing end but did not reorient or move towards the cathode.

Subsequent studies in the first half of the 20th century by a handful of researchers on various planarian species **(Table S1)** confirmed that intact planarians either orient and move towards the cathode (Hyman and Bellamy, 1922; Robertson, 1927; Hyman, 1932) or assume a U- or W-shape, which allowed them to bring their head and, for certain species future heads at fission locations, closest to the cathode, depending on the strength of the electric field (Hyman and Bellamy, 1922; Hyman, 1932). For *Dugesia tigrina*, Pearl's observation that the end of the planarian nearest the anode appears to contract was confirmed (Hyman and Bellamy, 1922; Robertson, 1927; Hyman, 1932). However, in contrast to Pearl's findings, all planarian fragments (heads, trunks, tails) were reported to exhibit cathodic electrotaxis (Robertson, 1927; Fries, 1928; Marsh and Beams, 1952; Viaud, 1952a).

Different mechanisms have been proposed to explain planarian electrotaxis: 1) Direct action of electrical current on nerve or muscle cells (Pearl, 1903; Fries, 1928), 2) an intrinsic bioelectric gradient in the body of the animal, with a positively charged head and a negatively charged tail (Hyman and Bellamy, 1922; Robertson, 1927; Hyman, 1932), 3) a bioelectric gradient with a negatively charged head and a positively charged tail that causes electrophoresis of a negatively charged diffusible head inhibitor molecule with source at the head (Lange and Steele, 1978), or 4) directional differences in conductance (with less resistance in the head) and excitation along the anterior-posterior axis (Viaud and Medioni, 1951; Viaud, 1952b, 1952a). The existing experimental data, however, are insufficient to distinguish among these theories. Furthermore, because different researchers used different planarian species, varying experimental conditions and manual scoring metrics, which were rarely described in detail and may have suffered from experimenter bias **(**reviewed by (Jenkins, 1967) and summarized in **Table S1)**, it is difficult to compile and interpret these previous findings. Therefore, we decided to revisit planarian electrotaxis with modern experimental tools and a quantitative and automated approach using the species *Dugesia japonica*, a popular species for planarian behavioral studies (Shomrat and Levin, 2013; Inoue, Yamashita and Agata, 2014; Inoue *et al.*, 2015; Sabry *et al.*, 2019; Zhang *et al.*, 2019; Ireland *et al.*, 2020; Le *et al.*, 2021). Experiments were conducted to test how various anatomical structures affect electrotaxis, to begin to differentiate between the proposed mechanisms.

Materials and Methods

Animal care

Asexual *Dugesia japonica* planarians were used for electrotaxis experiments. Planarians were kept in plastic containers filled with 0.5 g/L Instant-Ocean (IO) water (Spectrum Brands, Blacksburg, VA, USA) and stored at 18-20°C in temperature-controlled incubators (MIR-554, Panasonic, Kadoma, Osaka, Japan) in the dark when not used for experiments. Planarians were maintained following standard protocols (Dunkel, Talbot and Schötz, 2011), fed organic beef liver once a week, cleaned twice a week, and starved for at least one week before use in experiments.

Electrotaxis arena setup

We developed an arena in which five planarians can be simultaneously imaged during exposure to a static electric field, with computer-controlled voltage strength and field direction. We designed a 60.0 mm long trough arena with an isosceles trapezoid cross section shape. A trapezoidal shape was chosen to ensure that planarians can be observed even when moving along the container boundaries, for which they have a preference (Akiyama, Agata and Inoue, 2015). The trough is 17.3 mm wide at the top, 4.4 mm wide at the bottom, and 10.0 mm in height **(Figure 1A)**. Five troughs (arenas) were milled into a transparent acrylic sheet, allowing up to five independent experiments to be run simultaneously. Electrodes that take up the cross section of the arena were cut out of a 3 mm thick aluminum sheet and adhered with cyanoacrylate glue to either end of each arena.

The five sets of electrodes were arranged in a parallel circuit configuration. An external 18 Volt DC 2.0 Linear Bench Power Supply (CircuitSpecialists, Tempe, AZ, USA) provided a voltage to the circuit. A voltage was supplied to each arena through an 8-Channel 5 V Relay Shield Module Board Optocoupler Module Arduino ARM PIC AVR (Jekewin (Amazon), Seattle, WA, USA) which was controlled by an Arduino Uno **(Figure 1B)**. The 8-channel relay was connected to the aluminum electrodes and to the power supply by wires with alligator clips. All other connections were made using wires on a half-size breadboard (Adafruit Industries, New York, NY, USA).

To record experiments, a Basler Ace acA640 camera (Basler AG, Ahrensburg, Germany) was mounted on a ring stand above the arenas. Images were recorded at a rate of 8 frames per second as JPEG image stacks. Circuit control via the Arduino and recording via the Basler camera were controlled through MATLAB (version R2019b, MathWorks, Natick, MA, USA). The arenas were backlit with a 20 cm x 15 cm red electroluminescent panel (Adafruit Industries, New York, NY, USA) to provide contrast between the planarian and background **(Figure 1C)**. The output of the EL panel was measured with a Fieldmaster power meter (Coherent, Santa Clara, CA, USA), with an average power reading of 424 nW. Using Roscolux filters (#382;89;41;32; Rosco, NY), we estimated that the emission peak of the EL panel was between 600-700nm, a wavelength range planarians are insensitive to (Paskin *et al.*, 2014; Shettigar *et al.*, 2017) and in which they robustly respond to weaker stimuli, such as thermotaxis (Ireland *et al.*,

2020). All experiments were conducted with the room lights turned off. When filled with IO water with an applied voltage of 2 V, the arena would experience a voltage differential of 0.33 V/cm and an approximate current density of 0.077 mA/mm^2. IO water was measured with a conductivity meter (Traceable CC4360, VWR) to have a conductivity of ~780 µS/cm, or a resistivity of 12.8 Ωm.

Experimental conditions

Each arena was evenly filled with 4 mL of IO water. After filling the arenas with water, a background image of the entire setup was taken to be used for later data processing. One planarian was carefully dropped into the middle of each of the five troughs using a Samco 691 transfer pipet (Thermo Fisher Scientific, Waltham, MA, USA). Once all planarians were approximately centered in their arenas, planarians were exposed to the electric field and recorded. After half the predetermined experiment time elapsed, the electrical polarity was swapped **(Figure 1D)**. Recording was terminated and the voltage was brought to 0 V at the conclusion of each experiment. Planarians were subsequently removed from the arenas and placed in a recovery container. Prior to the beginning of another experiment, IO water was drained from each arena and arenas were wiped down with a paper towel to remove any mucus trails. All experiments were conducted at room temperature. For the voltage sweep, planarians were released approximately in the middle of their troughs at experiment onset **(Figure 1D)**. The experiment was 120 seconds in duration, with a polarity swap at 60 seconds (3 technical replicates with 5 planarians each in individual troughs for each voltage). To determine whether planarians responded to electrical current or to voltage, troughs were filled with 4 mL of either IO or ultrapure (Milli-Q; MQ) water. Experiments were run at 4 V for 90 seconds without a polarity swap. The higher voltage of 4 V was chosen to achieve: 1) a high voltage, high current condition (using IO water) and 2) a high voltage, low current condition (using ultra-pure water).

Temperature, convective currents, and pH tests

Temperature and pH differentials were measured when a 2 V electric field was applied to the arena, filled with 4 mL of IO water, for 360 seconds, with a polarity swap at 180 seconds (**SI Figure 1**). To measure temperature, an image of the arenas was taken before and after the electric field was applied using a FLIR infrared camera (FLIR Systems, Wilsonville, OR USA). We measured a negligible temperature gradient of ~0.5°C in our apparatus (which is within the 5% accuracy of the instrument). For reference, a gradient of ~8°C was required to induce thermotaxis in *Dugesia japonica* (Inoue, Yamashita and Agata, 2014). The pH was measured using pH test strips (Whatman, Maidstone, United Kingdom), and was found to be approximately 6.5 both before and after the electric field was applied. To test for convection, a drop of food coloring dye (Gel Spice Company Inc., Bayonne, NJ USA) was placed at the initial anode before a 2 V electric field was applied to an arena for 180 seconds, with a polarity swap at 90 seconds. As comparison, a drop of food coloring dye was placed in the same region of a different arena with a 0 V electric field. An image of the arenas was taken before and after the electric field was applied to visualize the convective currents through the dye movement.

Amputation experiments

For all experiments involving amputations, transverse amputations were used. To generate head and tail pieces, planarians were amputated either just above (pre-pharyngeal) or just below (post-pharyngeal) the pharynx using a sterile razor blade. For experiments involving trunk pieces, planarians were amputated both pre-pharyngeally and just below the auricles. For successive amputations, cuts transversally to the head-tail axis were administered in series. After each amputation, planarians were given at least one day to heal prior to conducting electrotaxis experiments. Because small tail pieces are less mobile than intact worms (Inoue, Yamashita and Agata, 2014; Inoue *et al.*, 2015), we increased the duration of the experiment when assessing post-pharyngeally cut tails. Head pieces and pre-pharyngeal tails were exposed to the electric field for 240 s, with an electrical polarity swap at 120 s; post-pharyngeal tails were exposed for 360 s with a polarity swap at 180 s.

Raw image data processing

Raw image data was imported into Fiji (Schindelin *et al.*, 2012) for background subtraction. The 5 arenas were separated into 5 image stacks using the rectangle tool to draw equal-sized rectangles around each arena and duplicating into individual image stacks. The arena background was subtracted from each of the five image stacks using the background image taken at the start of each experiment. The 5 stacks were then saved separately.

Data analysis and statistics

Processed frames were imported into MATLAB and binarized by manually setting a threshold that encompassed only the planarian. The center of mass of each planarian was then tracked in each frame using custom MATLAB code as previously described (Talbot and Schötz, 2011). The time spent in the arena quadrants and the fraction of time spent moving towards the cathodes for each planarian were outputted and compiled into a spreadsheet. To quantify the planarian's response to the electrical field, we calculated two parameters before ("1") and after ("2") the polarity swap. First, we calculated the fraction of time spent in the quadrant containing the cathode during the first or second half of the experiment ($f_{cat\text{-}1,2}$, time spent in cathode quadrant divided by total time with cathode at that location) and the fraction of time spent moving toward the cathode, $f_{mov\text{-}1,2}$. To determine the movement relative to the cathode, we only use the y-coordinate (1D motion). For each frame j in which the current COM coordinate y(j) is closer to the cathode position (set to y=0) than in the previous frame y(j-1), the planarian is scored as moving towards the cathode. The number of frames for which the planarian was scored as moving toward the cathode is then divided by the total number of frames for which the planarian is visible, yielding $f_{mov\text{-}1,2}$. When the planarian reaches the cathode, its COM is not recorded as the planarian is not visible to the program. Therefore, $f_{mov\text{-}1,2}$ complements $f_{cat\text{-}1,2}$, which measures the time spent at the cathode. If a planarian moves randomly, it is expected that on average it will spend equal amounts of time moving toward and away from the cathode. We did not set any thresholds, require persistence in motion or determine the velocity of motion, to avoid introducing additional parameters in the analysis. For trunk and tail pieces which are not as mobile and thus are less likely to reach the cathode, $f_{mov\text{-}1,2}$ is the most important parameter. The

fraction of experimental time spent in the middle two quadrants and in the anode quadrant (before and after the electrical polarity swap) were also recorded.

For length and area ratio measurements, the threshold method described above was used and the area and length of the body calculated using the built-in Analyze Particles function in Fiji. Head area and head length were manually measured by a researcher who was not involved in this project and thus naïve to the hypotheses, to prevent possible bias in the analysis. Ratios were calculated in MATLAB for visualization and in R (version 4.1.2, R Core Team) for statistical analysis. High magnification imaging of small and large planarians of the same size range as used for electrotaxis experiments was conducted to ensure that the analysis of the lower magnification images from the electrotaxis setup did not introduce any artifacts.

Responses to the electrical field were tested using analysis of variance (ANOVA) models. Response variables were proportions, either of trial time spent in the cathode zone or of trial time spent moving toward the cathode, before or after polarity swaps. Differences in these values between controls measured without a voltage applied and treatment group worms with a voltage applied constituted electrotaxis. For the initial test of electrotaxis at varying voltage levels, a one-way ANOVA was used with voltage as a predictor variable. Significant effects of voltage were followed up with Dunnett's post-hoc tests of 0 V controls against the non-zero voltages. Experiments with additional treatments were analyzed with factorial ANOVA. Since the difference between 0 V and 2 V was the indication of electrotaxis, the effect of other predictors (such as worm size) on electrotaxis was indicated by a significant interaction between voltage and the other predictors (that is, the amount of electrotaxis depends on worm size if the voltage x size interaction is significant). When significant interactions were detected the difference between 0 V and 2 V groups at the levels of the other predictor were used as post-hoc procedures, using Tukey's method to account for multiple comparisons. Post-hoc comparisons were only conducted following a significant ANOVA, so p-values for post-hoc comparisons of group means will be reported with the post-hoc procedure identified.

The successive cuts experiment used the same planarians with treatments that changed each day. These repeated-measures data were analyzed using the successive treatments as a within-subjects factor. The within-subjects treatments applied were different between two groups of worms, so the group was used as a between-subjects factor. The interaction of the within and

between-subjects factors indicated that the two groups differed in their responses to the two different treatment sequences. The same worms were tested at 0 V and 2 V to test for electrotaxis on each day, so post-hoc comparisons between the voltage levels were done with paired t-tests, and significance was assessed with a Bonferroni-adjusted alpha level (six comparisons were made, so p-values needed to be less than 0.05/6 = 0.008 to be considered statistically significant for the post-hoc paired t-tests).

Proportions often violate assumptions of normality and homoscedasticity, so these assumptions were tested prior to each analysis. When one or more assumptions were violated, we used non-parametric randomization tests to confirm that statistical significance of model terms was not affected. If significance was unchanged by using randomization tests, then post hoc procedures were conducted as usual, using either Tukey or Dunnett tests. All analysis was done with the R statistical computing language (version 4.1.2, R Core Team) and extension libraries. Post-hoc procedures were done with library emmeans (version 1.7.0). Randomization tests were done using library lmPerm (2.1.0). Homoscedasticity was tested with a Breusch-Pagan test from the lmtest library (0.9-38). Repeated measures analysis was done with the car library (3.0-11). The data, analysis in R and respective figures can be downloaded from the Collinslab github (https://github.com/Collinslab-swat/Planarian-electrotaxis).

Results

D. japonica exhibits cathodic electrotaxis at 2 V without overt adverse effects.

To determine what field strength was necessary to induce electrotaxis, we conducted a voltage sweep **(Table 1, SI Figure 2)**. At 0 V, planarians moved randomly and one would expect them to spend 25% of the experimental time in each quadrant. We found that they spent approximately 1/4-1/3 of the experimental time in the quadrants containing the cathode **(Table 1, SI Figure 2)**. The increased time spent in the quadrants containing the electrodes compared to the two middle quadrants likely results from planarians exhibiting wall preference (Akiyama, Agata and Inoue, 2015), as the electrode containing quadrants have more walls than the middle two quadrants **(Figure 1C, D)**. Planarians did not exhibit a preference for movement toward either electrode at 0 V; they moved toward and away from the cathode before and after polarity

swap at equal rates **(Table 1; SI Figure 2; Movie 1)**. When an electric field of 1 V was applied, planarians spent more time moving toward and staying in the cathode containing quadrants, but the increase was not significant compared to 0 V (Dunnett's test, $p = 0.587$). At 1.5-2 V, planarians reoriented themselves and moved toward the cathode **(Movie 1** shows planarian behavior at 2 V**)** and spent > 50% of the experimental time in the cathode-containing quadrants **(Table 1,** Dunnett's test, $p < 0.001$**)**. Planarians did not spend significantly more time moving toward the first cathode at 1.5 V but did so at 2 V and higher voltages **(Table 1,** Dunnett's test, $p = 0.16$ for 1.5 V, $p = 0.006$ for 2 V**,** $p < 0.001$ for 3 V and 4 V**)**. Once the polarity was swapped, planarians had a longer distance to move toward the new cathode because they predominantly started in the most distant quadrant, at cathode 1 **(Figure 1D)**. We observed that following the polarity swap, time moving towards cathode 2 ($f_{mov\text{-}2}$) appears to be a more consistent and sensitive measure for all voltages >1.5 V than time spent at the cathode **(**$f_{cat\text{-}2}$**), Table 1; SI Figure 2)**. This may be because planarians require longer to arrive at the second cathode from the most distant quadrant, causing time spent at the second cathode to be artificially low, whereas the time spent moving toward the cathode is relatively unchanged after the polarity swap.

While planarians exhibited electrotaxis at 3-4 V, they also exhibited vigorous head turning and oscillatory behavior **(Movie 2** shows planarian behavior at 4 V**)**. These behaviors caused the planarians to move more slowly toward the cathode. They still were able to reach the first cathode because they only had to traverse half of the trough but failed to reach the cathode after the polarity switch because they needed to travel the whole distance and the adverse effects increased over time. Because of these adverse effects at higher voltages, we conducted all further experiments at 2 V.

Next, we investigated whether the planarians sensed the electric field directly or they reacted to secondary effects induced by the field, such as gradients in pH, temperature, and convective currents, which can affect planarian behavior (Inoue, Yamashita and Agata, 2014; Ross *et al.*, 2018; Sabry *et al.*, 2020). We did not find significant effects of any of these factors (Methods; **SI Figure 1**). Thus, planarian movement toward the cathode is a direct response to the electric field.

To determine whether planarians responded to electrical current or to voltage, we tested the planarians' response to 4 V in either IO or ultrapure (MQ) water. Since the $f_{cat\text{-}2}$ parameter is not indicative of electrotaxis ability at 4 V as seen in **Table 1**, we calculated electrotaxis parameters without an electrical polarity swap. At 4 V, the current across a single trough of IO and ultra-pure water were measured to be 25.1 mA and 3.3 µA, respectively (averaged over 4 measurements). In IO water at 4 V, planarians spent significantly more time in the quadrant containing the cathode **(SI Figure 1C)** as well as spent more time moving towards the cathode compared to 0 V **(SI Figure 1D)**. The same trend was observed when planarians were placed in MQ water **(SI Figure 1C-D)**, demonstrating that planarian movement toward the cathode is not due to the electrical current (which differed by 4 orders of magnitude) but due to voltage. We will refer to this behavior as cathodic electrotaxis in subsequent sections.

Planarian body length affects cathodic electrotaxis ability

It has been previously shown that planarian behaviors such as locomotor velocity can be size dependent (Talbot and Schötz, 2011). To determine whether size also plays a role in planarian cathodic electrotaxis, experiments were run at 2 V on N=94 planarians that ranged in size from 2.0 - 12.4 mm. Planarians were classified as either "small", "medium", or "large" **(SI Figure 2B)**. Planarians in the large size class (7.6-12.4 mm) spent significantly more time at 2 V than at 0 V moving toward and staying in the quadrant containing the cathode, before and after the electrical polarity swap **(Figure 2A, B,** Tukey post-hocs, $p < 0.001$**)**. Planarians in the medium size class (4.6-7.5 mm) spent significantly more time at 2 V than at 0 V moving toward and staying near the first cathode **(Figure 2C, D,** Tukey post-hocs, $p < 0.003$**)**. After polarity reversal, medium sized planarians spent significantly more time moving towards the second cathode when voltage was applied (Tukey post-hocs, $p < 0.001$), although the time spent in the quadrant containing the second cathode was not significantly different between 0 V and 2 V **(Figure 2C**, Tukey post-hocs, $p = 0.077$**)**.

Small planarians (2.0-3.5 mm) spent significantly more time moving towards and staying near the first cathode at 2 V than at 0 V **(Figure 2E, F,** Tukey post-hocs, $p < 0.001$**)**. After the electrical polarity swap, small planarians spent significantly more time moving towards the second cathode (Tukey post-hocs, $p = 0.011$) but there was no difference in time spent in the

quadrant containing the second cathode **(Figure 2E, F**, Tukey post-hocs, p = 0.228**)**. This difference in behavior for smaller versus larger planarians was not due to differences in motility. While smaller planarians are known to move slower than larger planarians (Hagstrom *et al.*, 2015) and we observed differences in speed ((1.70 +/- 0.05) mm/s for large planarians and (1.02 +/- 0.04) mm/s for small planarians (mean +/- std); N= 30 and N=25, respectively), there was sufficient time (90 sec) for small planarians to travel the length of the trough (60 mm).

However, in contrast to large planarians, small planarians did not move toward the new cathode after the polarity swap but wandered around the anode containing quadrant **(Figure 2E** and **SI Figure 2C)**. Thus, small planarians do not exhibit the same electrotaxis behavior as large planarians. Besides differences in absolute size, we also found that differences in head size to body size exist between small and large planarians **(SI Figure 3).**

To determine the relationship between absolute size, relative head size, and the observed behavioral differences, and to characterize the role of specific anatomical structures, we took advantage of the regenerative abilities of planarians and compared electrotaxis in head, tail, and trunk fragments of various sizes.

Cathodic electrotaxis is a brain-independent behavior

To test whether cathodic electrotaxis requires key anatomical structures, such as the head, tail, auricles, and pharynx, we bisected planarians into head and tail pieces either anterior to (pre-) or posterior to (post-) the pharynx **(Figure 3 A,B)**. Amputated planarians were allowed one day to heal before assaying for electrotaxis ability. If electrotaxis ability was solely size dependent and not influenced by other factors, we would expect to find that larger fragments electrotax more robustly than smaller ones, independent of their head or tail identity. However, we found that tail pieces retained the ability to electrotax independent of size **(**Tukey post-hocs, $p < 0.001$; **SI Figure 3A**), whereas head pieces did not exhibit cathodic electrotaxis regardless of amputation location **(Figure 3 C-E; SI Figure 3A).** Moreover, the time-colored trajectories of head and tail pieces (**Figure 3C**) show that the most striking behavioral difference between heads and tails occurs after the polarity swap, when the first cathode becomes the new anode, and the pieces need to traverse the entire trough to reach the new cathode. While head

trajectories look similar at 0V and 2V, tail trajectories are distinctively different, with straighter trajectories at 2V, that begin at the new anode and end at the new cathode, demonstrating electrotaxis.

As planarian tail pieces lack brains yet still maintain the ability to electrotax, these results demonstrate that the planarian brain or the auricles are not required for electrotaxis. Furthermore, because tail pieces with and without the pharynx electrotaxed **(SI Figure 4**), these experiments show that the pharynx is not required for cathodic electrotaxis. Moreover, small post-pharyngeal tails electrotaxed more robustly than larger pre-pharyngeal heads **(Figure 3E)**.

Because tail fragments, especially smaller ones, exhibit lower motility compared to head fragments, which affects the time spent at the cathodes (Methods; (**Figure 3C,D**) and because the behavior at the cathodes is also influenced by other factors, such the planarians' wall preference behavior (Akiyama, Agata and Inoue, 2015), the time spent at the cathode is a less suitable parameter to assay electrotaxis than the motility parameters $f_{mov\text{-}1,2}$. Because behavioral differences were most pronounced after the polarity swap (**Figure 3C-E**) when planarians needed to traverse the entire trough to get to the cathode, we focused on f_{mov2} for all further analyses.

The relative size of the head to the body affects electrotaxis

Our experiments on cut planarians showed that tail fragments exhibit electrotaxis independent of their size, whereas size affects electrotaxis ability in head fragments, with larger fragments (post-pharyngeally cut heads) retaining some electrotaxis ability but smaller (pre-pharyngeally cut heads) not exhibiting electrotaxis (**Figure 3**). Given these data and the observed size effects in intact planarians (**Figure 2, SI Figure 2**), we hypothesized that the relative size of the head to the size of the body (i.e. the total size) may affect electrotaxis.

To investigate a possible relationship between electrotaxis ability and head size/body size, we took head length and body length, and head area and body area measurements and calculated head size/body size for both metrics for the pre-pharyngeally and post-pharyngeally cut heads (Methods; **Figure 4A**)**.** We found a significant interaction between head proportion and time spent moving towards the second cathode ($f_{mov\text{-}2}$) for both metrics at 2V but not at 0V

(Figure 4B, C). Head fragments with relatively smaller heads showed stronger electrotaxis, supporting the hypothesis that the relative size of the head affects electrotaxis ability.

Taken to the extreme, these data suggest that removal of the head should be able to restore electrotaxis in a head fragment that cannot electrotax. Thus, we dissected the role of the head for the electrotaxis ability of individual planarians.

Head removal restores electrotaxis behavior in planarian fragments

First, we quantified electrotaxis in pre-pharyngeal heads and trunks **(SI Figure 5)**. These animals were exposed to a 2 V electric field for 240 s with a polarity swap at 120 s. We then decapitated the heads, removed an equivalent tissue fragment from the anterior end of the trunks, and re-evaluated electrotaxis after 24 h, to allow for healing. We found that pre-pharyngeal heads do not electrotax, but this ability is restored by decapitation **(SI Figure 5).** Because one could argue that (a) the planarians may have differed in their ability to electrotax from the beginning and (b) that any anterior cut may restore electrotaxis, we repeated this experiment using successive cuts on large planarians with tracking of individual animals that we verified to have electrotaxis ability. Planarians were cut post-pharyngeally, allowed to heal for 24 h, and split into two groups **(Figure 5A)**. Subsequently group 1 had a small amount of tissue removed from the posterior end and group 2 was cut pre-pharyngeally. On day 2, both groups were again assessed for electrotaxis, after which group 1 was cut pre-pharyngeally and had a small amount of tissue removed from the tip of the nose while group 2 was decapitated. On day 3, both groups were assessed for a final time **(Figure 5A)**. Members of group 1 retained a head throughout the experiment, whereas members of group 2 lost their head in the third amputation. Each group received the same number of posterior and anterior cuts, to account for any changes that may be introduced by amputation.

We found that post-pharyngeally cut heads (day 1) showed no electrotaxis, consistent with earlier experiments. Within Group 1, post-pharyngeal heads with an additional posterior wound (day 2) showed weak electrotaxis. Pre-pharyngeal amputation coupled with an anterior wound (day 3) caused loss of electrotaxis **(Figure 5B)**. Similarly, within group 2, pre-pharyngeal heads (day 2) failed to show electrotaxis. However, trunk pieces formed by subsequent

decapitation (day 3) showed clear recovery of electrotaxis **(Movie 3)** with statistically significant changes in both $f_{mov\text{-}1}$ and $f_{mov\text{-}2}$ **(Figure 5C)**. A non-decapitating anterior wound (Group 1) did not restore electrotaxis. Based on these results, we conclude that it is the presence or absence of a head that is the strongest factor determining planarian cathodic electrotaxis.

Discussion

Using an automated experimental setup that minimizes experimenter bias and other external influences, our data show that the apparent electrotactic response by planarians is in fact due to the electric field rather than to other environmental cues. This is an important distinction to make as planarians are known to sense temperature and chemical gradients (Inoue, Yamashita and Agata, 2014; Inoue *et al.*, 2015) and electric fields in water can generate thermal, pH, and convective effects (Gunji and Washizu, 2005; May and Hillier, 2005). While these ancillary effects of the method used to generate static electrical fields should be minimal given the small voltage applied, it was important to test for them as it is unclear how sensitive planarians are. The voltages in previous studies (Pearl, 1903; Hyman and Bellamy, 1922; Robertson, 1927; Fries, 1928; Hyman, 1932), whether directly reported or estimated based on current and arena dimensions **(SI Table 1)**, are much larger than the 2 V we used in our experiments, and are less likely to have isolated the effects of the electric field from other associated environmental changes.

The high and variable voltages involved in previous studies likely account for some of the variability in the reported results, as well as the observed dramatic behaviors such as planarians curling up on their sides (Hyman and Bellamy, 1922; Hyman, 1932), scrunching (Robertson, 1927), paralysis and death (Pearl, 1903). These prior studies largely assumed that the response was elicited by current (Pearl, 1903; Hyman and Bellamy, 1922; Robertson, 1927; Fries, 1928; Hyman, 1932) **(SI Table 1)**. The finding that planarians electrotax similarly in both ionized and deionized water despite a current difference of 4 orders of magnitude demonstrates that *D. japonica* planarians sense and respond to voltage and not to electrical current. The distinction between voltage and current informed our subsequent experimental design and is key to future efforts to determine the mechanism underlying planarian electrotaxis.

We showed that electrotaxis is not tied to a specific anatomical structure via amputation experiments. We assayed the role of the brain and sensory structures such as the auricles and pharynx, which are used in chemotaxis (Asano *et al.*, 1998; Miyamoto *et al.*, 2020). Pre-pharyngeally cut tail fragments lack the brain and auricles, while post-pharyngeally cut tail fragments also lack the pharynx. The presence of electrotactic behavior in both types of tail fragments shows that the brain, pharynx, and auricles are not required. Thus, voltage sensing, and subsequent directed motion cannot be attributed to specific anatomical structures but rather depends on a broadly distributed or graded property throughout the body. In addition, our voltage sweep showed that cathodic electrotaxis does not result from direct electrical action on either the cilia or muscles, because we were able to elicit the behavior in planarians gliding (1.5-2 V) and using musculature-driven locomotion (scrunching) (3-4 V).

Our observation that electrotaxis is weaker in smaller worms is interesting, as smaller planarians do not represent a different life stage where certain structures or tissues might be absent or immature. However, our results from varying sizes of both intact planarians and fragments show that electrotaxis ability is not a direct consequence of size **(SI Figure 3A)**. Instead, we found that differences in head size to body size exist between small and large planarians **(SI Figure 3 B, C)** and that the relative size of head to body correlates with electrotaxis ability (**Figure 4**). Strikingly, a fragment containing a head lacks the ability to electrotax, whereas a similarly sized fragment without a head retains this ability. This finding is the opposite of what was reported in the literature for other planarian species **(Table SI 1)**, wherein it was found that head pieces in an electric field behaved more like intact planarians than other fragments (Pearl, 1903; Fries, 1928).

Behavioral differences among species are known to exist for other stimulated behaviors (Ireland *et al.*, 2020) and it is possible that the electrotaxis response of *D. japonica* differs from the other planarian species previously studied. An alternative explanation is that our use of lower field strength to avoid the adverse effects of electric field exposure described in the literature (scrunching, curling, paralysis, death (Pearl, 1903; Hyman and Bellamy, 1922; Robertson, 1927; Hyman, 1932)) elicited more differentiated behaviors.

Previous work on planarian electrotaxis has attributed the worms' reaction to electric fields to direct action of the electric current on the muscles (Pearl, 1903; Fries, 1928), intrinsic bioelectric gradients of the animal (Robertson, 1927; Hyman, 1932; Lange and Steele, 1978) or head-to-tail differences in electrical conductance (Viaud and Medioni, 1951; Viaud, 1952a). Lange & Steele proposed an electrochemical model for axial patterning and measured the intrinsic bioelectric gradient. They reported that the head was negatively charged relative to the body, with a posteriorly increasing positive charge toward the tail (Lange and Steele, 1978). Based on these data, they proposed that the head-to-tail bioelectric gradient caused electrophoresis of a negatively charged head inhibitor molecule that is produced in the brain. Thus, according to their model, there exists a static bioelectric gradient superimposed by a dynamic concentration gradient of a negatively charged morphogen that travels head to tail. Upon decapitation, a piece whose bioelectric gradient was aligned with an external electric field would thus experience a positive anterior relative to its posterior and migrate toward the cathode, as observed in the classical patterning experiments by Marsh & Beams (Marsh and Beams, 1952) (**Figure 6**).

Conversely, Hyman proposed that the bioelectric gradient correlates with a metabolic gradient and because the head was more metabolically active, the head region was positively charged compared to the body (Hyman, 1932) (**Figure 6**). Recent work (Durant *et al.*, 2017) using the DiBAC4(3) voltage reporter (Oviedo *et al.*, 2008) showed that the very tip of the head region is relatively depolarized (positively charged). While this result seems to support Hyman's model, it does not directly contradict the measurements of Steele & Lange, given the coarse nature of their measurements and the observation that most of the head does not appear depolarized in the DiBAC experiments. DiBAC experiments also showed that trunk pieces have polarity with anterior wounds being more positively charged than posterior wounds (Durant *et al.*, 2019), in agreement with both model predictions and the observed cathodic electrotaxis (Marsh and Beams, 1952).

A fourth explanation for electrotaxis was provided by Viaud & Medioni who reported that electrical conductance and excitation was consistently greater and the threshold for a response to current was lower when the planarian's head was facing the cathode than when it faced the anode (Viaud and Medioni, 1951). This observation was reproduced in head and tail

fragments (Viaud, 1952a). Thus, this model makes similar behavioral predictions as the Hyman model.

How do these different explanations perform in the light of our experimental data? We can rule out the direct action of current on the musculature as the driving force for electrotaxis because we were able to elicit electrotaxis at 2 V without musculature driven locomotion. The models that propose anterior-posterior bioelectric or conductance gradients similarly cannot explain all the data (**Figure 6**).

While all models can explain the observed cathodic electrotaxis of trunk and tail fragments, the Hyman and Viaud models would predict head fragments to equally move toward the cathode, which was not observed in our experiments. The Lange & Steele model would predict intact planarians and head fragments to move toward the anode, given the presumed negative charge of the planarian head and constant production of a negatively charged morphogen in the head; however, this was also not observed in our experiments. Thus, none of the current models can explain all of our data.

One may question why we see electrotaxis in intact planarians but not in post-pharyngeally cut head fragments. This can be explained by the difference in head to body ratio, which we have shown to affect electrotaxis ability **(Figure 4)**. What distinguishes the head from the rest of the planarian body is the presence of a brain consisting of many different types of neurons organized in a bilobed neuronal network (Cebrià *et al.*, 2002; One Pagan, 2014). Viaud already proposed that differences in head and tail current sensitivity and excitation anisotropy may result from the quantity and type of neurons in each fragment (Viaud, 1952a) and suggested that the animal orients itself in the electrical field to maximize neuronal excitation. In trunk and tail fragments, the ventral nerve cords run parallel to the anterior-posterior axis, and thus could promote alignment with the external field. In contrast, neuronal connections in the head extend in all directions (as seen from the center of the head); thus, there may not be a preferred direction of orientation and no electrotaxis is observed. While it is possible that the commissures (smaller bundles of nerves that branch off perpendicular to the ventral nerve cords) also play a role in electrotaxis, our data show that if commissures play a role, their effect does not seem to dominate the response; else we would expect head fragments to also electrotax, as they contain many commissures.

The finding that planarian electrotaxis is a brain-independent behavior differs from electrotaxis in other invertebrates, where it is mediated by specific neurons in the head. The nematode *Caenorhabditis elegans* moves towards the cathode in response to electric fields (Shanmugam, 2017), and this behavior is disrupted when amphid sensory neurons in the head ganglia are surgically severed (Gabel *et al.*, 2007; Salam *et al.*, 2013; Chrisman *et al.*, 2016). In *Drosophila* larvae, a subset of peripheral neurons in the terminal organ at the anterior tip of the head become strongly activated when the neuronal axis becomes aligned with the direction of electric field (Riedl, 2013). In contrast, our results show that neurons in the head are not required for planarian electrotaxis; instead, their presence seems to impair the behavior. The quantitative data and methods presented here lay the foundation for future studies to dissect how headless planarian fragments sense electric fields, and to determine how inhibitory signals from the head impair cathodic electrotaxis.

Acknowledgments

The authors thank Veronica Bochenek for help with planarian care, Maia Chandler and Yianni Krontiris for the head and body size image analysis, Dr. William Kristan Jr. and Dr. Alex Mogilner for discussions, and Tapan Goel, Dr. Danielle Ireland, and Dr. William Kristan Jr. for comments on the manuscript.

Funding

This work was funded by NSF CAREER Grant 1555109 (to EMSC) and Swarthmore College. The funders had no role in the design and conduct of the study, in the collection, analysis, and interpretation of the data, and in the preparation, review, or approval of the manuscript.

References

Akiyama, Y., Agata, K. and Inoue, T. (2015) 'Spontaneous Behaviors and Wall-Curvature Lead to Apparent Wall Preference in Planarian', *PLOS ONE*, 10(11), p. e0142214.

Asano, Y. *et al.* (1998) 'Rhodopsin-like proteins in planarian eye and auricle: Detection and functional analysis', *Journal of Experimental Biology*, 201(9), pp. 1263–1271.

Cebrià, F. *et al.* (2002) 'The expression of neural-specific genes reveals the structural and molecular complexity of the planarian central nervous system', *Mechanisms of Development*, 116(1–2), pp. 199–204. doi: 10.1016/S0925-4773(02)00134-X.

Chrisman, S. D. *et al.* (2016) 'C. elegans demonstrates distinct behaviors within a fixed and uniform electric field', *PLoS ONE*, 11(3). doi: 10.1371/journal.pone.0151320.

Cochet-Escartin, O., Mickolajczk, K. J. and Collins, E.-M. S. (2015) 'Scrunching: a novel escape gait in planarians', *Physical Biology*, 12(5), p. 055001. doi: 10.1088/1478-3975/12/5/056010.

Currie, K. W. and Pearson, B. J. (2013) 'Transcription factors lhx1/5-1 and pitx are required for the maintenance and regeneration of serotonergic neurons in planarians.', *Development (Cambridge, England)*, 140(17), pp. 3577–88. doi: 10.1242/dev.098590.

Dunkel, J., Talbot, J. and Schötz, E. M. (2011) 'Memory and obesity affect the population dynamics of asexual freshwater planarians', *Physical Biology*, 8(2). doi: 10.1088/1478-3975/8/2/026003.

Durant, F. *et al.* (2017) 'Long-Term, Stochastic Editing of Regenerative Anatomy via Targeting Endogenous Bioelectric Gradients', *Biophysical Journal*, 112(10), pp. 2231–2243. doi: 10.1016/j.bpj.2017.04.011.

Durant, F. *et al.* (2019) 'The Role of Early Bioelectric Signals in the Regeneration of Planarian Anterior/Posterior Polarity', *Biophysical Journal*, 116(5), pp. 948–961. doi: 10.1016/j.bpj.2019.01.029.

Fries, E. F. B. (1928) 'Drug action in galvanotropic responses', *Journal of General Physiology*, 11(5), pp. 507–513. doi: 10.1085/jgp.11.5.507.

Gabel, C. V. *et al.* (2007) 'Neural Circuits Mediate Electrosensory Behavior in Caenorhabditis elegans', *Journal of Neuroscience*, 27(28), pp. 7586–7596. doi: 10.1523/JNEUROSCI.0775-07.2007.

Goel, T. *et al.* (2021) 'Let it rip: the mechanics of self-bisection in asexual planarians determines their population reproductive strategies.', *Physical biology*, 19(1). doi: 10.1088/1478-3975/ac2f29.

Gunji, M. and Washizu, M. (2005) 'Self-propulsion of a water droplet in an electric field', *Journal of Physics D: Applied Physics*, 38(14), pp. 2417–2423. doi: 10.1088/0022-3727/38/14/018.

Hagstrom, D. *et al.* (2015) 'Freshwater planarians as an alternative animal model for neurotoxicology', *Toxicological Sciences*, 147(1), pp. 270–285. doi: 10.1093/toxsci/kfv129.

Hyman, L. H. (1932) 'Studies on the Correlation between Metabolic Gradients, Electrical Gradients, and Galvanotaxis. II. Galvanotaxis of the Brown Hydra and Some Non-Fissioning Planarians', *Physiological Zoology*, 5(2), pp. 185–190. doi: 10.1086/physzool.5.2.30152783.

Hyman, L. H. and Bellamy, A. W. (1922) 'Studies on the correlation between metabolic gradients, electrical gradients, and galvanotaxis', *Biological Bulletin*, 43(5), pp. 313–347.

Inoue, T. *et al.* (2015) 'Planarian shows decision-making behavior in response to multiple stimuli by integrative brain function', *Zoological Letters*, 1(1), pp. 1–15. doi: 10.1186/s40851-014-0010-z.

Inoue, T., Yamashita, T. and Agata, K. (2014) 'Thermosensory signaling by TRPM is processed by brain serotonergic neurons to produce planarian thermotaxis.', *The Journal of neuroscience : the official journal of the Society for Neuroscience*, 34(47), pp. 15701–14. doi: 10.1523/JNEUROSCI.5379-13.2014.

Ireland, D. *et al.* (2020) 'Dugesia japonica is the best suited of three planarian species for high-throughput toxicology screening', *Chemosphere*, p. 2020.01.23.917047. doi: 10.1101/2020.01.23.917047.

Jenkins, M. M. (1967) 'Aspects of Planarian Biology and Behavior', *Chemistry of Learning*, pp. 117–143. doi: 10.1007/978-1-4899-6565-3_9.

Lange, C. S. and Steele, V. E. (1978) 'The Mechanism of Anterior-Posterior Polarity Control in Planarians', *Differentiation*, 11(1–3), pp. 1–12. doi: 10.1111/j.1432-0436.1978.tb00965.x.

Le, D. *et al.* (2021) 'Planarian fragments behave as whole animals', *Current Biology*. doi: 10.1016/J.CUB.2021.09.056.

Malinowski, P. T. *et al.* (2017) 'Mechanics dictate where and how freshwater planarians fission', *Proceedings of the National Academy of Sciences of the United States of America*, 114(41), pp. 10888–10893. doi: 10.1073/pnas.1700762114.

Marsh, G. and Beams, H. W. (1952) 'Electrical control of morphogenesis in regenerating dugesia tigrina. I. Relation of axial polarity to field strength', *Journal of Cellular and Comparative Physiology*, 39(2), pp. 191–213. doi: 10.1002/jcp.1030390203.

May, E. L. and Hillier, A. C. (2005) 'Rapid and reversible generation of a microscale pH gradient using surface electric fields', *Analytical Chemistry*, 77(19), pp. 6487–6493. doi: 10.1021/ac051014w.

Miyamoto, M. *et al.* (2020) 'The pharyngeal nervous system orchestrates feeding behavior in planarians', *Science Advances*, 6(15), pp. 1–10. doi: 10.1126/sciadv.aaz0882.

Nishan, S. *et al.* (2021) 'Discovery of a body-wide photosensory array that matures in an adult-like animal and mediates eye–brain-independent movement and arousal', *Proceedings of the National Academy of Sciences*, 118(20), p. e2021426118. doi: 10.1073/pnas.2021426118.

One Pagan (2014) *The First Brain: The Neuroscience of Planarians*. First edit. Oxford University Press.

Oviedo, N. J. *et al.* (2008) 'Live Imaging of Planarian Membrane Potential Using DiBAC4(3).', *CSH protocols*, 2008, p. pdb.prot5055. doi: 10.1101/pdb.prot5055.

Paskin, T. R. *et al.* (2014) 'Planarian Phototactic Assay Reveals Differential Behavioral Responses Based on Wavelength.', *PloS one*, 9(12), p. e114708. doi: 10.1371/journal.pone.0114708.

Pearl, R. (1903) 'The Movements and Reactions of Fresh-water Planarians: A Study in Animal Behaviour; The Quarterly Journal of Microscopical Science', *The Quarterly Journal of Microscopical Science*, 46, pp. 509–714. doi: 10.1126/science.17.436.737.

Riedl, J. (2013) *Identification of neurons controlling orientation behavior in the Drosophila melanogaster larva*.

Rink, J. C. (2018) 'Stem cells, patterning and regeneration in planarians: Self-organization at the organismal scale', in *Methods in Molecular Biology*. Humana Press Inc., pp. 57–172. doi: 10.1007/978-1-4939-7802-1_2.

Robertson, J. A. (1927) 'Galvanotropic Reactions of Polycelis nigra in Relation to Inherent Electrical Polarity', *Journal of Experimental Biology*, 5(1), pp. 66–88.

Rompolas, P., Patel-King, R. S. and King, S. M. (2010) 'An outer arm dynein conformational switch is required for metachronal synchrony of motile cilia in planaria', *Molecular Biology of the Cell*, 21(21), pp. 3669–3679. doi: 10.1091/mbc.E10-04-0373.

Ross, K. G. *et al.* (2018) 'SoxB1 Activity Regulates Sensory Neuron Regeneration, Maintenance, and Function in Planarians', *Developmental Cell*, 47(3), pp. 331-347.e5. doi: 10.1016/j.devcel.2018.10.014.

Sabry, Z. *et al.* (2019) 'Pharmacological or genetic targeting of Transient Receptor Potential (TRP) channels can disrupt the planarian escape response', *PLoS ONE*, p. 753244. doi: 10.1101/753244.

Sabry, Z. *et al.* (2020) 'Planarian scrunching as a quantitative behavioral readout for noxious stimuli sensing', *Journal of Visualized Experiments*. doi: 10.3791/61549.

Salam, S. *et al.* (2013) 'A microfluidic phenotype analysis system reveals function of sensory and dopaminergic neuron signaling in C. elegans electrotactic swimming behavior', *Worm*, 2(3), p. e24558. doi: 10.4161/worm.24558.

Schindelin, J. *et al.* (2012) 'Fiji: An open-source platform for biological-image analysis', *Nature Methods*, 9(7), pp. 676–682. doi: 10.1038/nmeth.2019.

Shanmugam, M. M. (2017) 'Galvanotaxis of Caenorhabditis elegans: current understanding and its application in improving research', *Biology, Engineering and Medicine*, 2(1), pp. 1–5. doi: 10.15761/bem.1000111.

Shettigar, N. *et al.* (2017) 'Hierarchies in light sensing and dynamic interactions between ocular and extraocular sensory networks in a flatworm', *Science Advances*, 3(7), p. e1603025. doi: 10.1126/sciadv.1603025.

Shomrat, T. and Levin, M. (2013) 'An automated training paradigm reveals long-term memory in planarians and its persistence through head regeneration', *The Journal of Experimental Biology*, 216(20), pp. 3799 LP – 3810. doi: 10.1242/jeb.087809.

Talbot, J. and Schötz, E. M. (2011) 'Quantitative characterization of planarian wild-type behavior as a platform for screening locomotion phenotypes', *Journal of Experimental Biology*, 214(7), pp. 1063–1067. doi: 10.1242/jeb.052290.

Viaud, G. (1952a) 'Anisotropie d'excitation galvanique et anisotropie électrique de segments et de pharynx isoles de Planaria (Dugesia) lugubris O. Schm.', *Comptes rendus des séances de la Société de biologie et de ses filiales*, 146(17–18), pp. 1382–1384.

Viaud, G. (1952b) 'Anisotropie électrique et variations de la conductance en fonction de la taille chez Planaria lugubris O. Sch.', *Comptes rendus des séances de la Société de biologie et de ses filiales*, 146(5–6), pp. 489–492.

Viaud, G. and Medioni, J. (1951) 'Anisotropie d'excitation et variations des seuils de réaction au courant galvanique en fonction de la taille chez Planaria lugubris, O. Sch.', *Comptes rendus des seances de la Societe de biologie et de ses filiales*, 145(15–16), pp. 1228–31.

Zhang, S. *et al.* (2019) 'Multi-behavioral endpoint testing of an 87-chemical compound library in freshwater planarians', *Toxicological Sciences*, (1), pp. 26–44.

Figures and Table

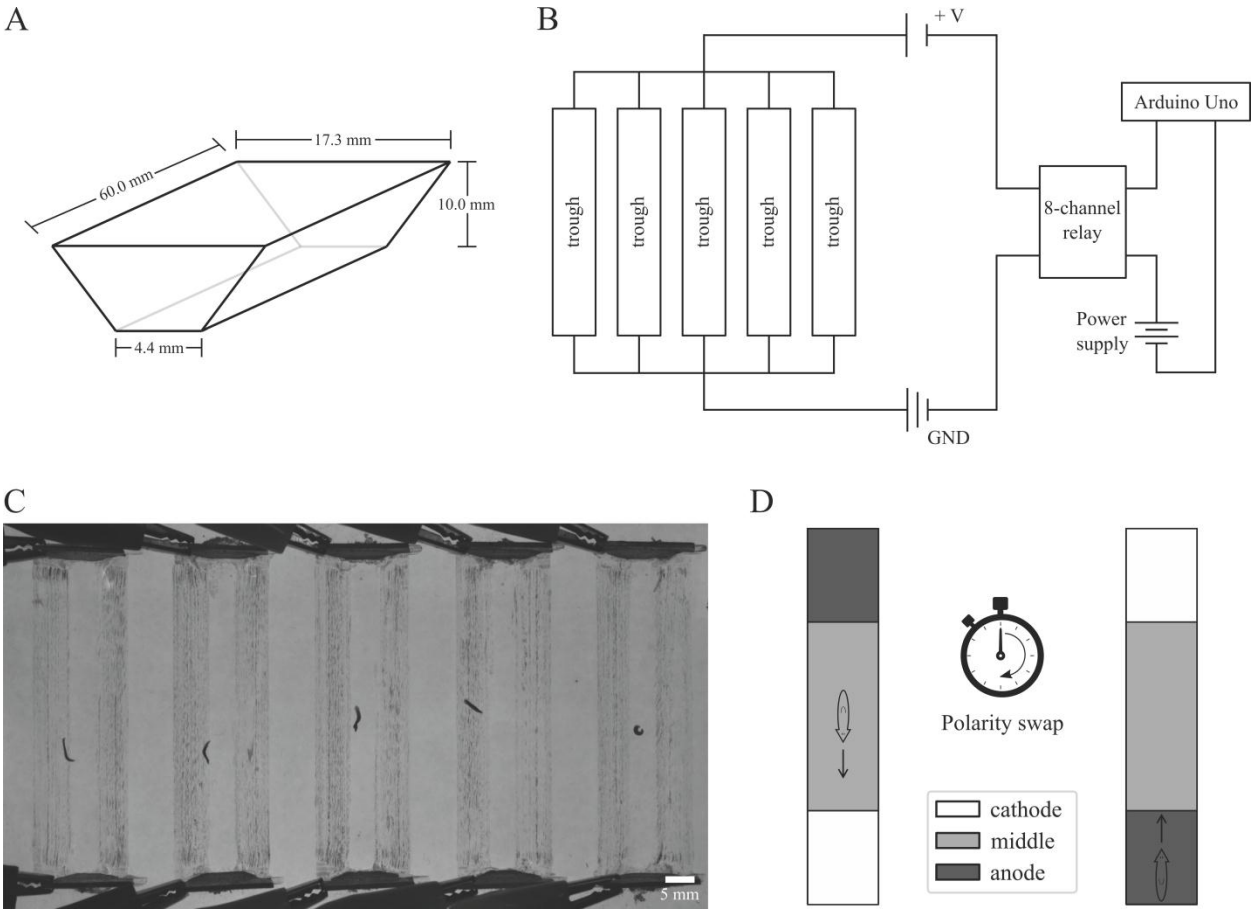

Fig. 1. Schematics of planarian electrotaxis setup. (A) Schematic of one trough (arena) with an isosceles trapezoidal cross-section. (B) Circuit diagram of electrotaxis setup. (C) Representative image of planarians in the arenas backlit with a red electroluminescent panel. (D) Schematic showing a planarian in an arena. Planarians were dropped in the middle of each trough at the start of the experiment. The electrical polarity was reversed after half the experiment time had elapsed. White, grey, and dark-grey regions denote the cathode quadrant, middle two quadrants, and anode quadrant, respectively.

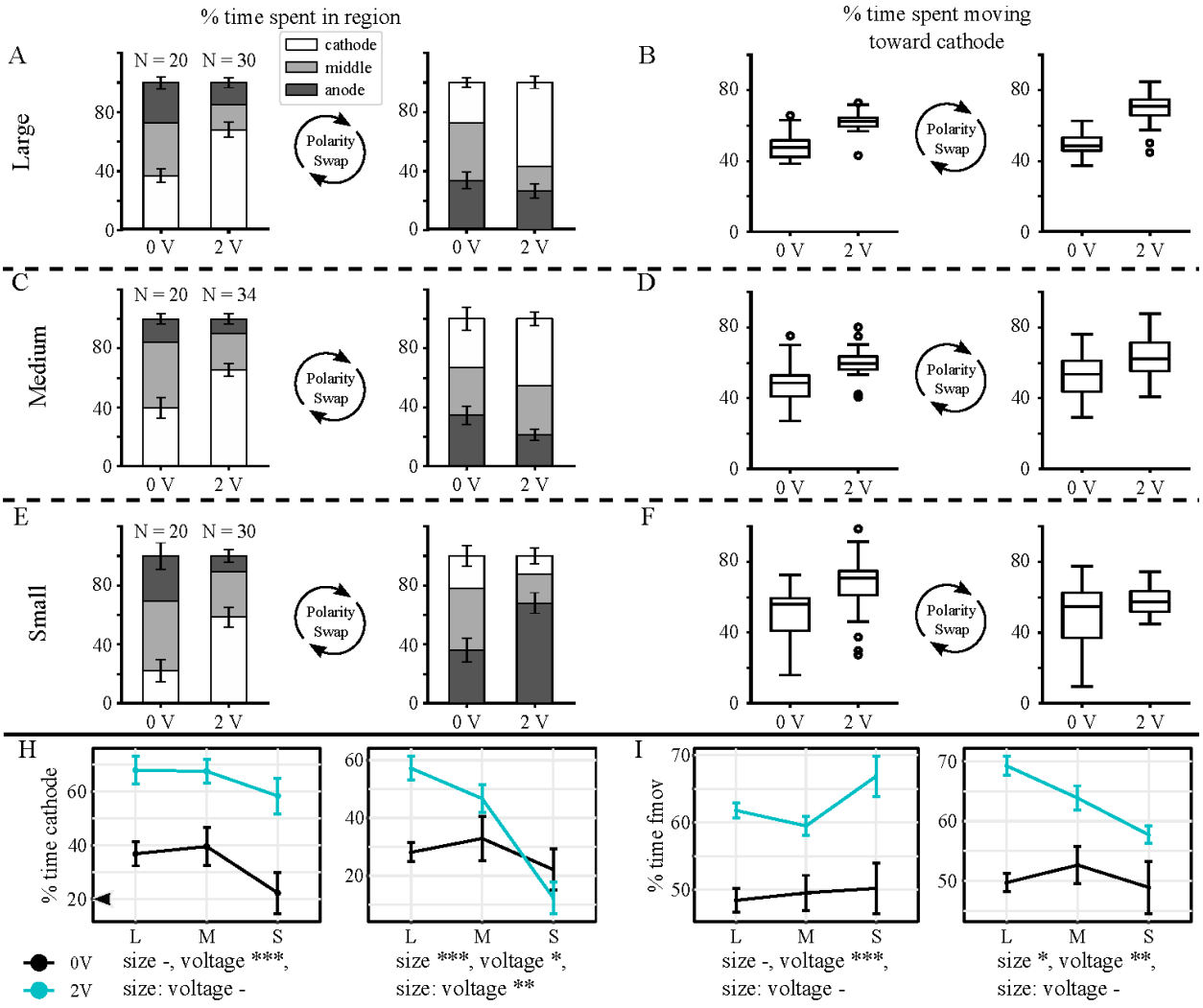

Fig. 2. Size and electrotaxis ability. (A, C, E) Segmented bar plots showing the percent experiment time, before and after the electrical polarity swap, spent in the cathode quadrant, anode quadrant, and middle two quadrants for (A) large, (C) medium, and (E) small sized planarians. Error bars denote standard error. (B, D, F) Box-and-whisker plots showing the percentage of experiment time, before and after the electrical polarity swap, spent moving toward the cathode for (B) large, (D) medium, and (F) small sized planarians. Open circles denote outliers. G. Interaction plots showing % time spent at the cathode for small, medium, and large planarians at 0 V and 2 V, before and after electrical polarity swap. H. Interaction plots showing % time moving towards the cathode for small, medium, and large planarians at 0 V and 2 V, before and after electrical polarity swap and the effect of planarian size (length) and voltage.

"size: voltage" refers to interactions of size and voltage. *** denotes $p < 0.001$, ** denotes $p < 0.01$, * denotes $p < 0.05$, - denotes $p > 0.05$. Shown are mean values and error bars denote standard error.

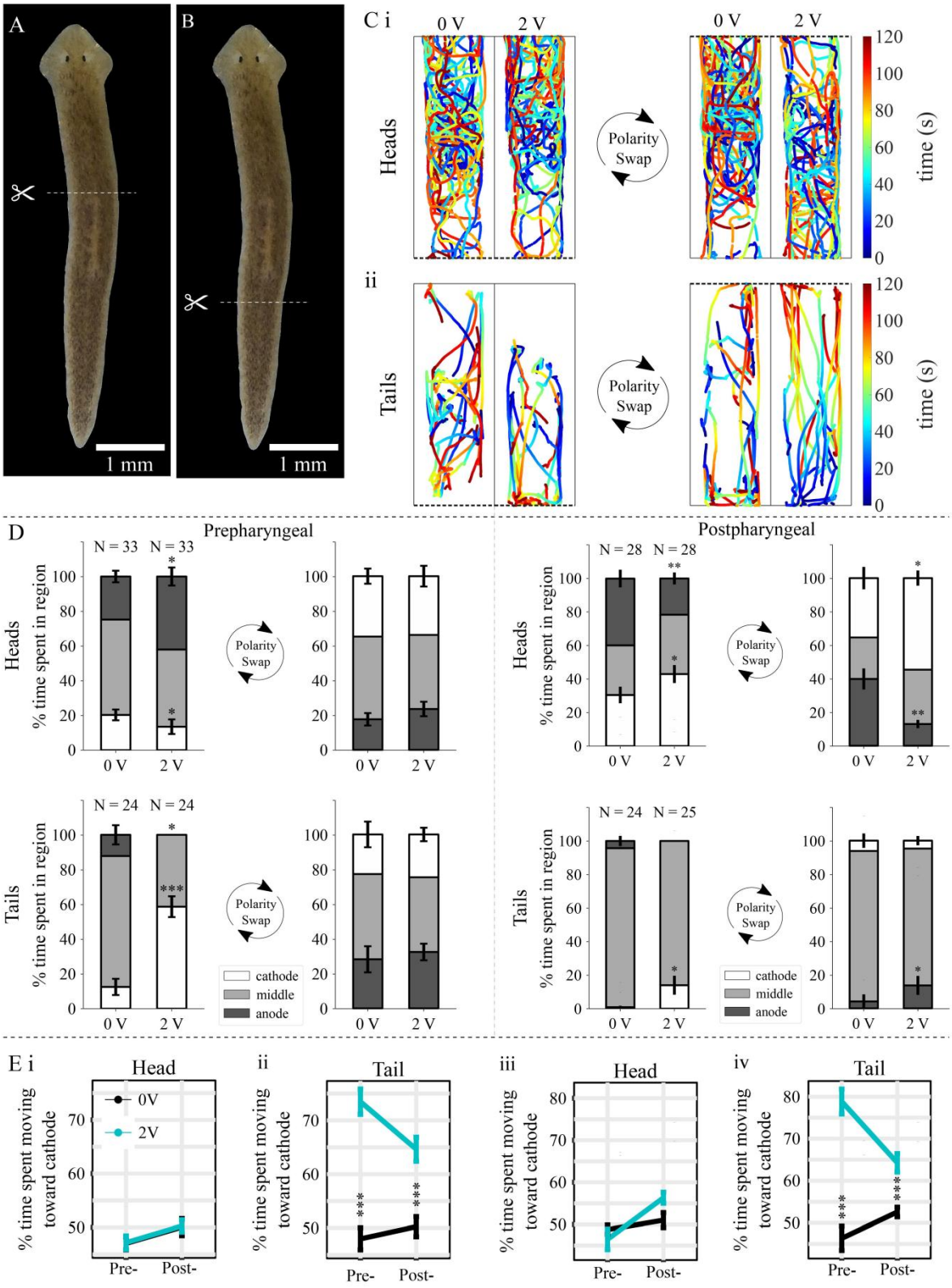

Fig. 3. Electrotaxis behavior of head pieces but not of tail pieces depends on cut location. (A) Schematic showing the site of pre-pharyngeal amputations. Pharynx location indicated by bracket; auricles indicated by white arrows. (B) Schematic showing the post-pharyngeal cut location. (C) Paths traveled for a subset of N = 15 pre-pharyngeally cut (top) Head and (bottom) Tail planarians exposed to a 0 V or 2 V electric field. Dashed lines denote the location of the cathode. Heads move randomly at both 0V and at 2V, whereas tails show a preference for the cathode containing quadrant. (D) Segmented bar plots showing the percent experiment time, before and after the electrical polarity swap, spent in the cathode quadrant, anode quadrant, and middle two quadrants. Error bars denote standard error. (E) Comparisons of time spent moving towards the cathode for pre- and post-pharyngeal head and tail fragments. i, ii. Before polarity swap, iii, iv. After polarity swap. * denotes $p < 0.05$, ** denotes $p < 0.01$, and *** denotes $p < 0.001$ from the respective 0 V controls as calculated using Tukey post-hoc comparisons. Tukey post-hocs, $p = 0.378$ for pre-pharyngeally amputated pieces, $p = 0.063$ for post-pharyngeally amputated pieces. Shown are mean values and error bars denote standard error.

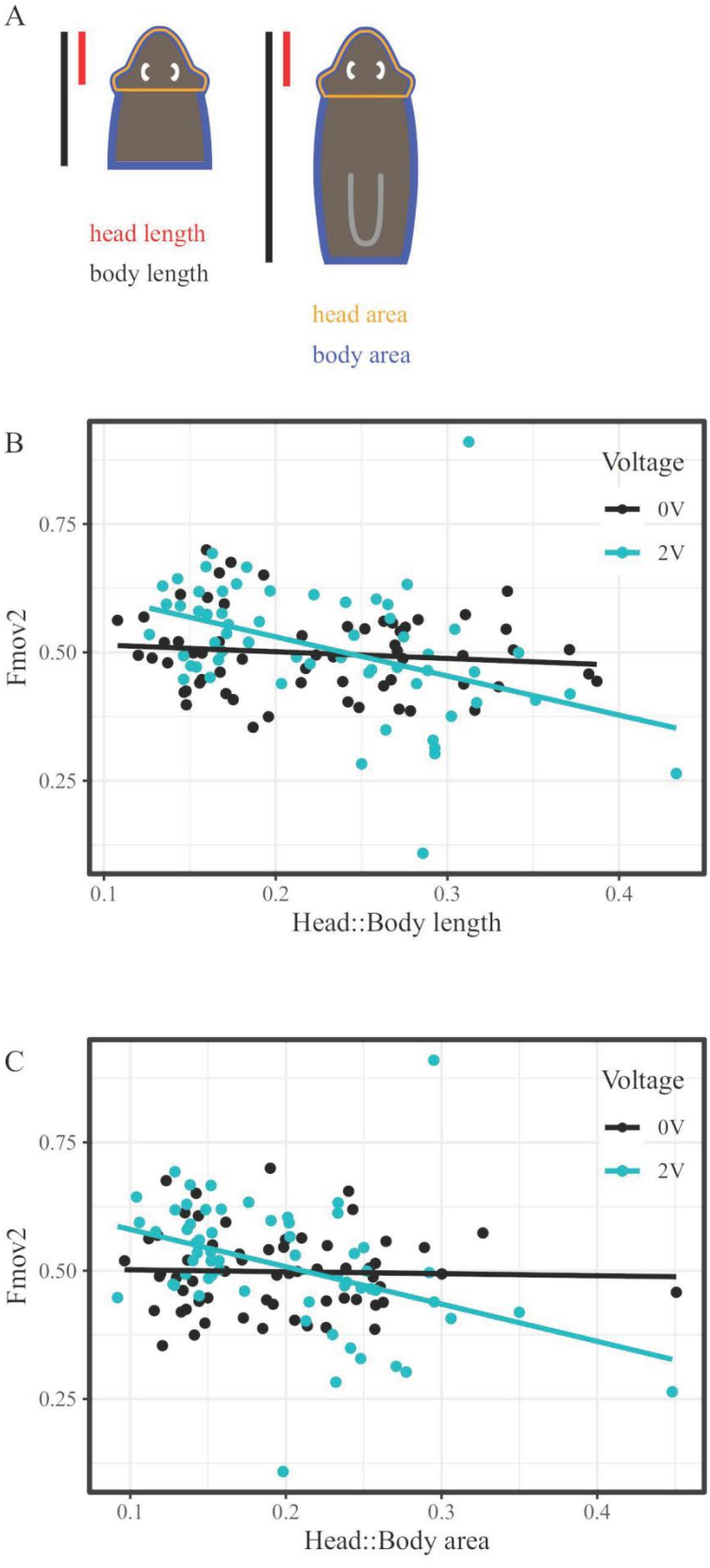

Fig. 4. Head proportion affects electrotaxis behavior. (A) Schematic showing pre-pharyngeal (left) and post-pharyngeal (right) head fragments and calculation of head proportion. For length, the red (head) and black (body) lengths were measured. For area, the outlined regions (orange: head; blue: body) were measured. (B) Interaction plots between head length to body length ratio and time spent moving towards second cathode. (C) Interaction plots between head area to body area ratio and time spent moving towards second cathode. Both plots show increased movement toward the second cathode with a decrease in head/body ratio at 2V but not at 0V, with the effect being more pronounced for area ratios.

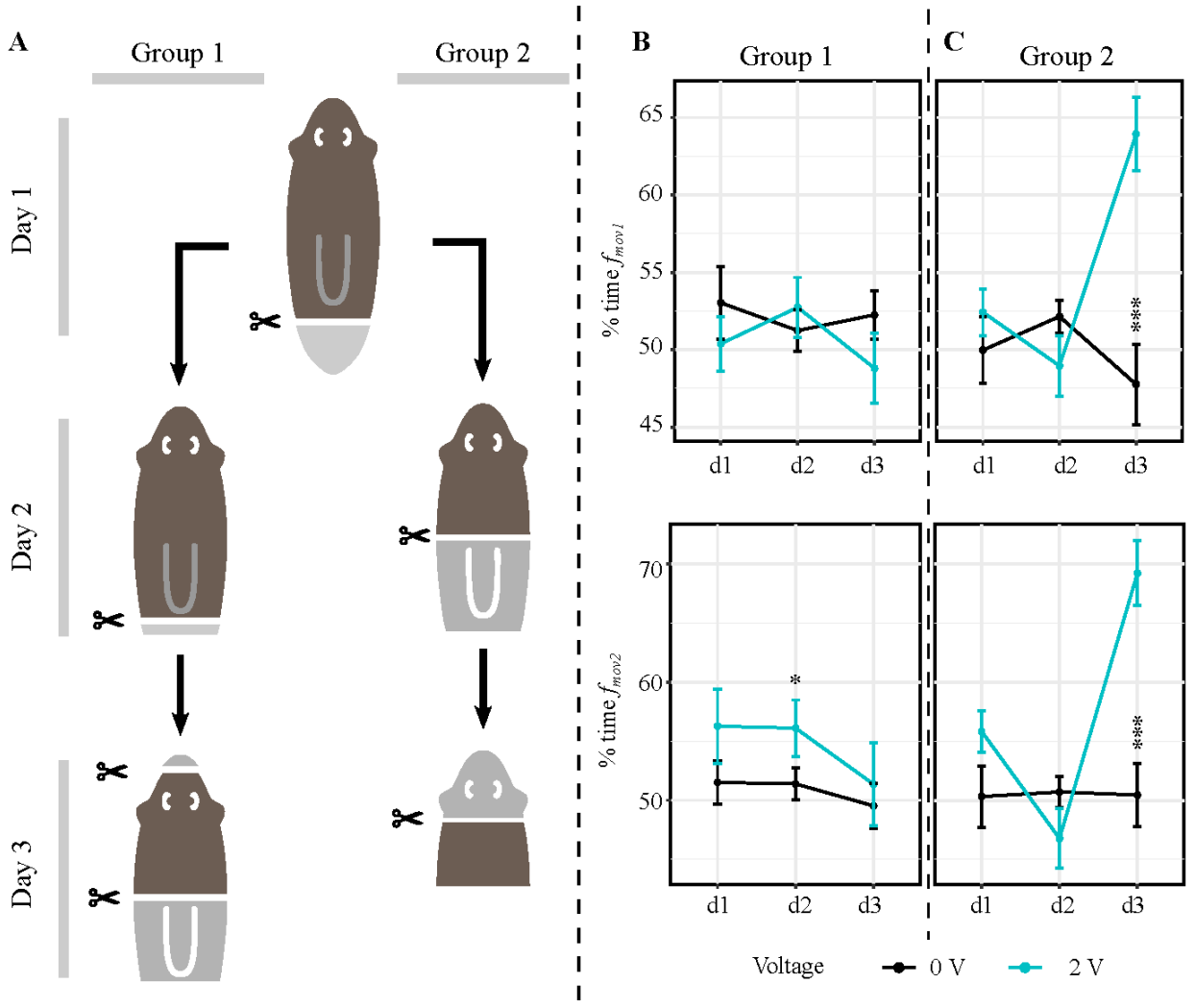

Fig. 5. Electrotaxis metrics are dependent on presence or absence of a head. A. Schematic of experimental procedure. Notably, the indicated cuts were performed the day prior to the experimental day indicated in the text. B. Time spent moving towards the cathode on each day, Group 1. C. Time spent moving towards the cathode on each day, Group 2. * denotes $p < 0.05$, ** denotes $p < 0.01$, and *** denotes $p < 0.001$ from the respective 0 V controls as determined by post hoc comparisons. Shown are mean values and error bars denote standard error.

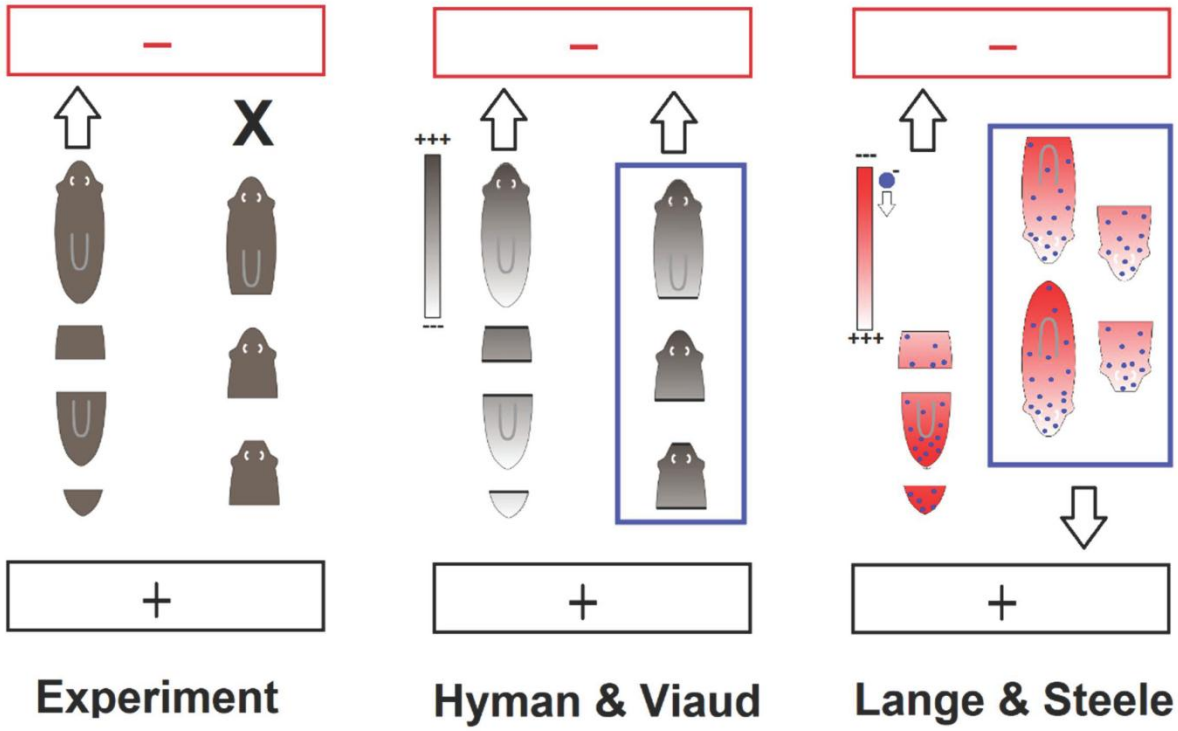

Fig. 6. Testing proposed models against our experimental data. The cathode is indicated in red and the anode in black. Left: Results obtained in our experiments. Cathodic electrotaxis is indicated by an arrow, lack of electrotaxis is indicated by X. Middle: The Hyman & Viaud models partially explain the data but would predict cathodic electrotaxis of head fragments which was not observed in experiment. Right: The Lange & Steele model partially explain the data but would predict anodic electrotaxis of intact planarians and head fragments which was not observed in experiment. The blue boxed cases highlight which experimental data is not explained by each model.

Table 1. Parameters for baseline experiments. For each voltage tested, N=15 planarians (6.4 mm – 11.1 mm in length) were used in 3 experimental replicates with N=5. Voltage values are reported to ± 0.01 V; current values are averages of 4 measurements. Electrotaxis parameter values are reported as mean ± standard error. * denotes $p < 0.05$, ** denotes $p < 0.01$ and *** denotes $p < 0.001$ differences from the 0 V control using Dunnett's post-hoc comparisons.

Voltage	Current	$f_{cat\text{-}1}$	$f_{mov\text{-}1}$	$f_{cat\text{-}2}$	$f_{mov\text{-}2}$
0 V	0 A	0.22 ± 0.06	0.49 ± 0.03	0.36 ± 0.04	0.51 ± 0.03
1 V	0.03 mA	0.33 ± 0.06	0.53 ± 0.02	0.39 ± 0.04	0.55 ± 0.02
1.5 V	4.4 mA	0.64 ± 0.07***	0.56 ± 0.02	0.56 ± 0.03**	0.63 ± 0.02**
2 V	8.4 mA	0.65 ± 0.07***	0.63 ± 0.02***	0.54 ± 0.05*	0.72 ± 0.01***
3 V	16.6 mA	0.80 ± 0.04***	0.76 ± 0.03***	0.10 ± 0.05***	0.72 ± 0.02***
4 V	25.1 mA	0.72 ± 0.06***	0.79 ± 0.03***	0.08 ± 0.03***	0.88 ± 0.02***

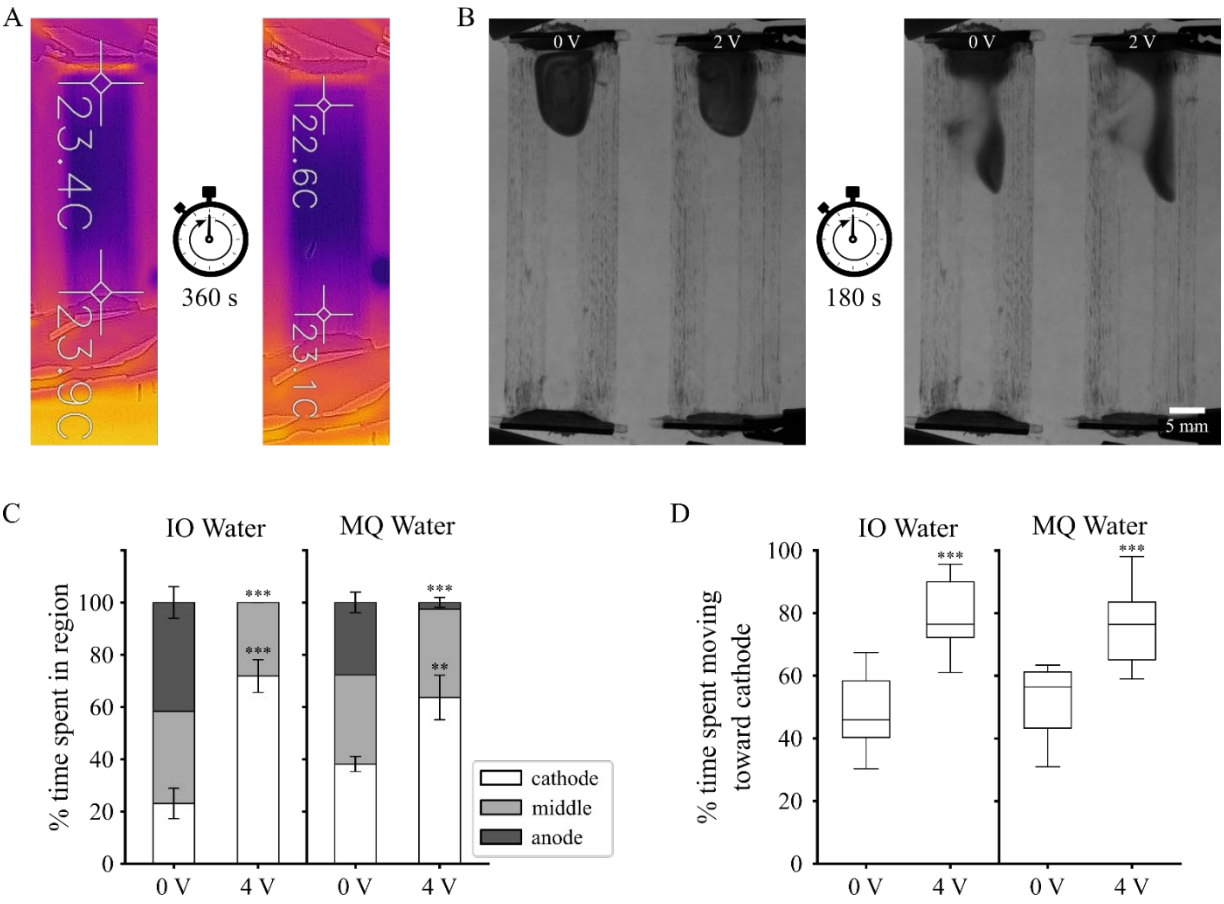

Fig. S1. Electrotaxis is not a consequence of temperature gradients, convection, or current. (A) Infrared images of a trough arena filled with 4 mL of IO water taken before (left) and after (right) a 2 V electric field was applied for 360 s. The measured temperature difference between the electrodes is 0.5C before and after, which is within the noise of the measurement. (B) Images taken of dye in trough arenas before (left) and after (right) 180 s of either 0 V or 2 V. (C) Bar graphs showing the average percent experiment time planarians spent in the cathode or anode quadrants or the middle two quadrants at 0 V and 4 V in IO or ultrapure (MilliQ; MQ) water. Error bars denote standard error. (D) Box-and-whisker plots showing the percent experiment time planarians spent moving toward the cathode. (C-D) N = 15 planarians were placed in IO or MQ water at 0 V or 4 V. ** denotes $p < 0.01$ and *** denotes $p < 0.001$ from factorial ANOVA. The interaction between water type and voltage was not statistically significant for either C or D.

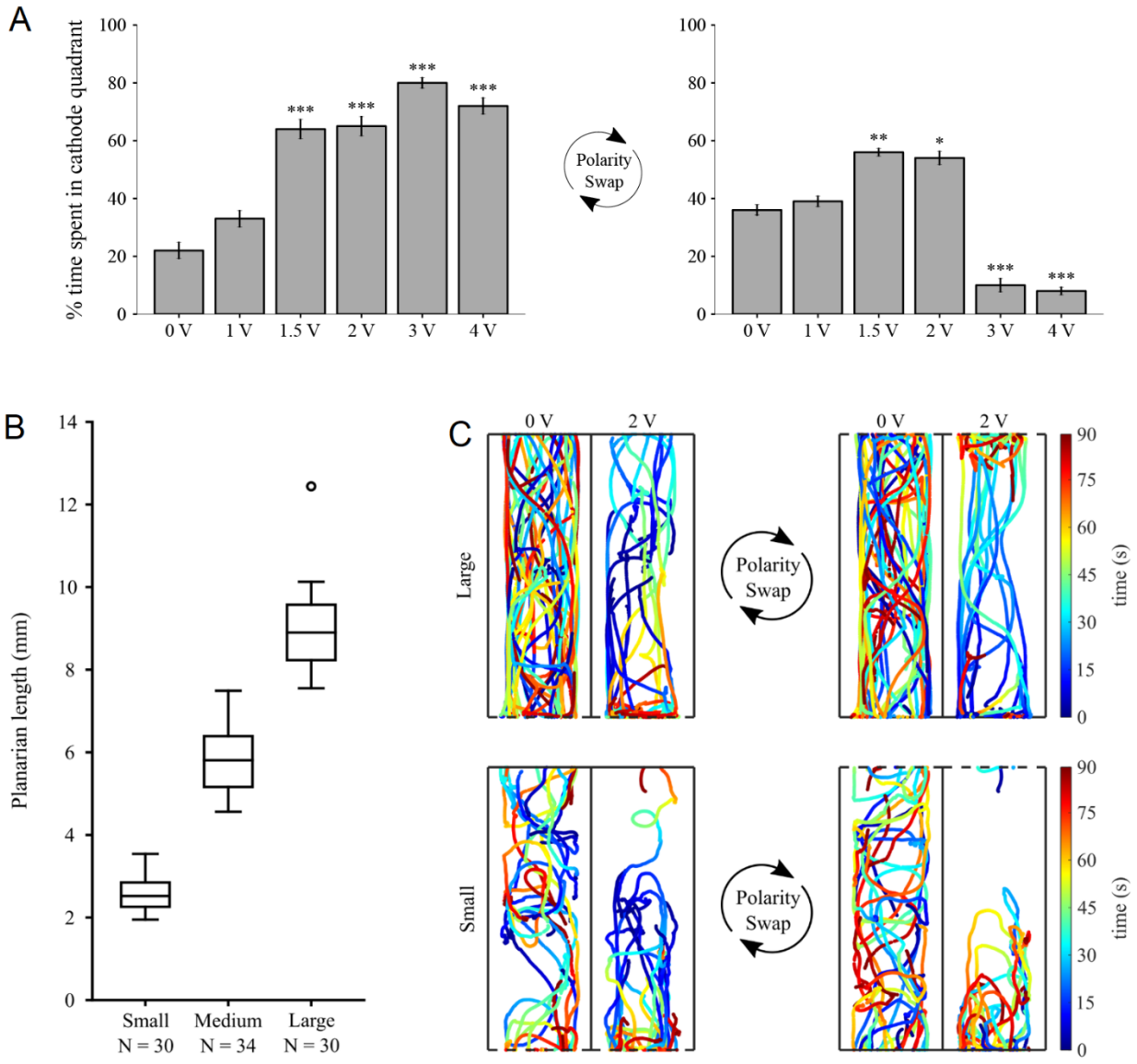

Fig. S2. Voltage and size dependence of planarian movement in the electric field. (A) Bar plots showing the percentage of experimental time spent in the quadrant containing the cathode before (left) and after (right) the electrical polarity swap. Bar height denotes mean percent experimental time and error bars denote standard error. * denotes $p < 0.05$, ** denotes $p < 0.01$ and *** denotes $p < 0.001$ differences from the 0 V control using Dunnett's post-hoc comparisons. N=15 planarians (6.4 mm – 11.1 mm in length) were used in 3 replicates with N=5 per experiment. (B) Box-and-whisker plots showing the size distributions of planarians in the small, medium, and large size classes. (C) Paths traveled for a subset of N = 15 (top) large and (bottom) small planarians exposed to a 2 V electric field for 180 s with a polarity swap occurring at 90 s. Dashed lines denote the location of the cathode electrode.

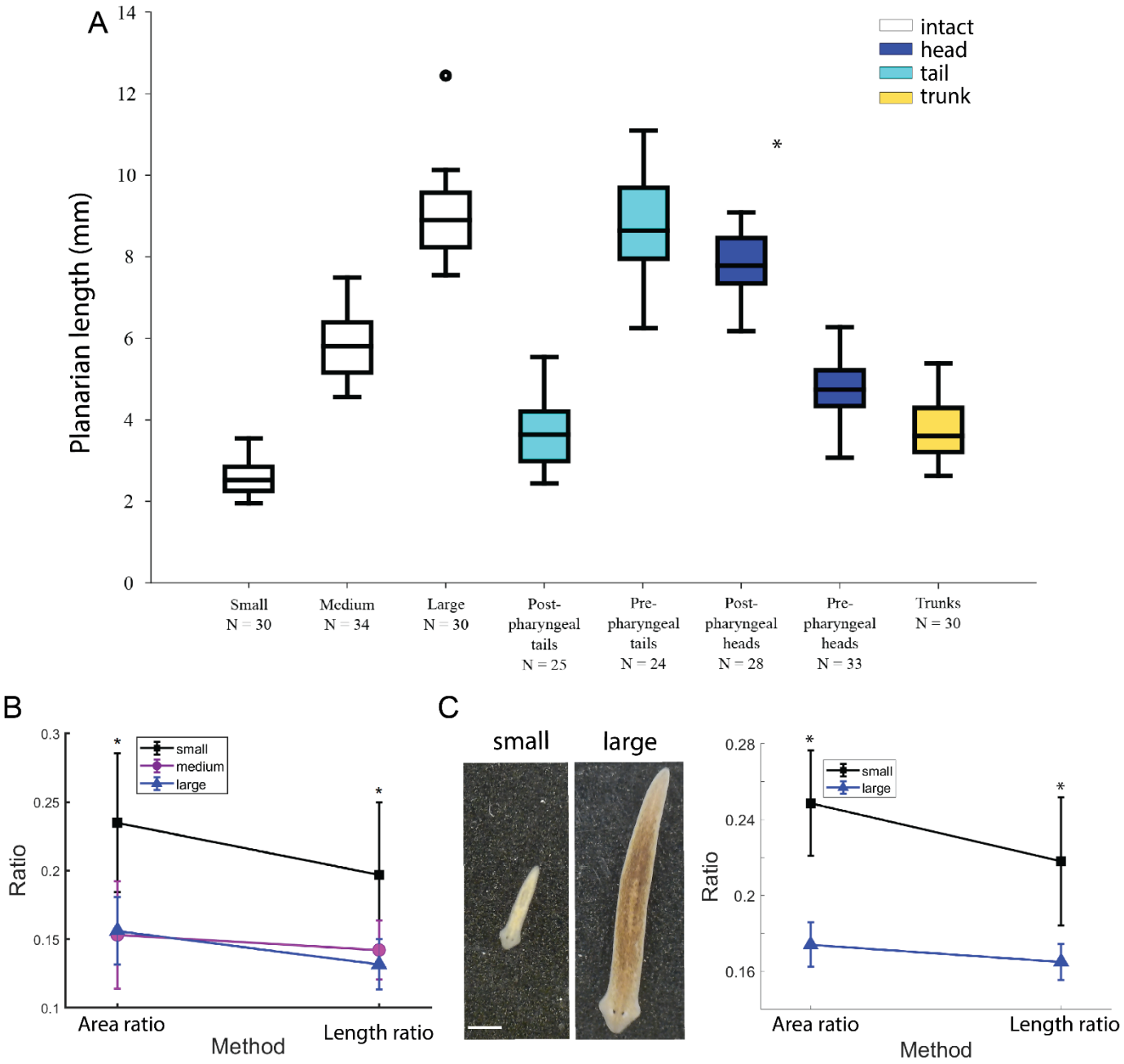

Fig. S3. Lengths and head-to-body ratios of planarians used in electrotaxis experiments. (A) Box-and-whisker plot showing the lengths of representative subsets of planarians used in the different experiments. Fragments are color coded by type. Open circles denote outliers. (B) For planarians used in electrotaxis experiments, there was a significant difference ($p < 0.05$) in head-to-body-ratio between small and medium, and small and large planarians, as measured by length and by area. There was no difference between medium and large planarians. (C) Representative images of small and large planarians from high magnification imaging, which was used to confirm the observed differences in head-to-body-ratio from the lower resolution data from the electrotaxis setup. High magnification data also shows that there is a difference between length ratios and area ratios for small but not for large planarians, implying that any comparisons using length ratios is an underestimation of the differences between the two groups. Scale bar: 1mm.

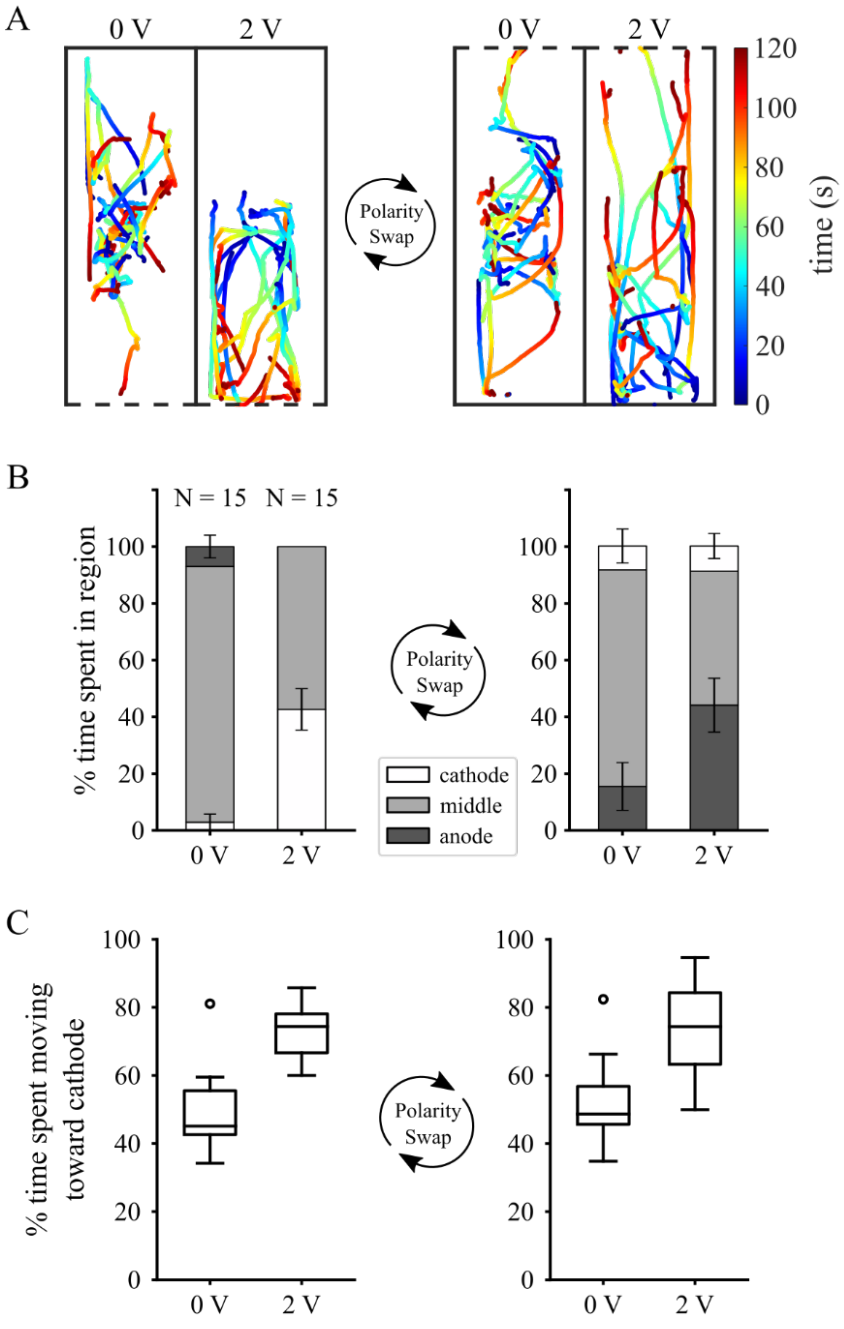

Fig. S4. Removal of the pharynx does not disrupt electrotaxis ability in pre-pharyngeally cut tail pieces. (A) Paths traveled for N = 15 pre-pharyngeally cut planarian tail pieces with pharynges removed. Dashed lines represent the location of the cathode. (B) Segmented bar plots showing the percent experiment time, before and after the electrical polarity swap, spent in the cathode quadrant, anode quadrant, and middle two quadrants. Error bars denote standard error. (C) Box-and-whisker plots showing the percentage of experiment time, before and after the electrical polarity swap, spent moving toward the cathode. Open circles denote outliers. Although 0V and 2V groups differ for all comparisons, the interaction between voltage and pharynx treatment was not significant for any (factorial ANOVA).

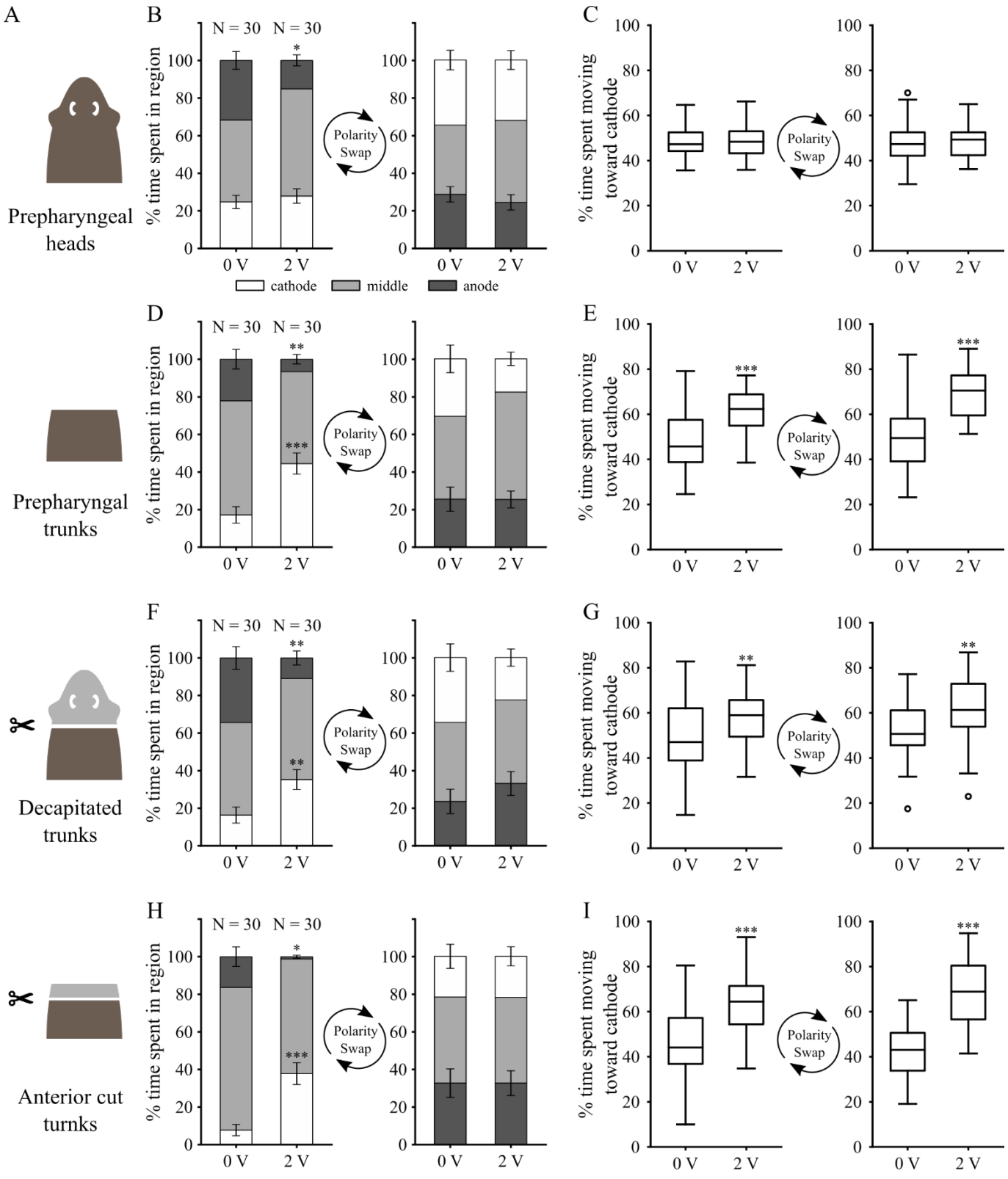

Journal of Experimental Biology • Supplementary information

Fig. S5. Decapitation of pre-pharyngeally cut head pieces restores cathodic electrotaxis ability. Animals were exposed to a 2 V electric field for 240 s with a polarity swap at 120 s. (A) Schematics illustrating planarian fragments and cutting process. The grey colored region was first removed, then the brown colored piece was tested for electrotaxis ability 24 hours later. (B, D, F, H) Segmented bar plots showing the percent experiment time, before and after the electrical polarity swap, spent in the cathode quadrant, anode quadrant, and middle two quadrants for (B) pre-pharyngeally cut head pieces (D) pre-pharyngeally cut trunk pieces, (F) pre-pharyngeally cut head pieces that have been decapitated and, (H) pre-pharyngeally cut trunk pieces that have had an anterior cut. Error bars denote standard error. (C, E, G, I) Box-and-whisker plots showing the percentage of experiment time, before and after the electrical polarity swap, spent moving toward the cathode for (C) pre-pharyngeally cut head pieces (E) pre-pharyngeally cut trunk pieces, (G) pre-pharyngeally cut head pieces that have been decapitated and, (I) pre-pharyngeally cut trunk pieces that have had an anterior cut. Open circles denote outliers. * denotes $p < 0.05$, ** denotes $p < 0.01$ and *** denotes $p < 0.001$ from the respective 0 V controls using the statistical analyses described in Methods.

Table S1. Summary of existing planarian electrotaxis literature. Jenkins (Jenkins 1967) reviews several of these older studies in more detail.

Reference	Species	Electrical parameters	Amputated worms	Cathodic electrotaxis	Behavior	Proposed mechanism
(Pearl 1903)	*Planaria maculata (=Dugesia tigrina), dorotocephala, gonocephala*	n/a	Y	Observed in intact worms and anterior pieces but not tails	Head turning towards cathode, crawling (=scrunching), curling at high current	Stimulation of muscle fibers oriented parallel to the current
(Hyman & Bellamy 1922)	*Planaria maculata (=Dugesia tigrina),* Unidentified triclad	110V DC generator w/variable resistor	N	Y	Curling with ventral side, head and tail towards cathode	Bioelectric gradient resulting from metabolic gradient; with head more positive than tail
(Robertson 1927)	*Polycelis nigra*	1.5-10mA DC	Y	Y in all conditions; longitudinally cut worms and head/trunk/tail fragments	Gliding, crawling (=scrunching)	Electric gradient; same orientation as proposed by Hyman
(Fries 1928)	*Planaria maculata (=Dugesia tigrina), planaria agilis (=Dugesia dorotocephala)*	0.3-0.5mA, 5V or less	Y	Y for untreated worms and head and tail fragments, reversed with strychnine	Turning, some movement, contraction of end near electrode	Direct stimulation of nerves or muscles by current
(Hyman 1932)	*Planaria dorotocephala*, *Curtisia foremanii* (= *Planaria simplissima*), *Procotyla fluviatilis* (= *Dendrocoelum lacteum*)	~1mA, 5-20V	N	Y	Crawling (=scrunching), turning, U- and W-shaped curling on side	Bioelectric gradient, with head more positive than tail
(Marsh & Beams, 1952)	*Dugesia tigrina*	Current densities 1.6-24.4 $\mu A/mm^2$	Y	Y	Movement of fragments toward cathode; no intact planarians tested	Inherent polarity of cut pieces
(Viaud & Medioni 1951)	*Dugesia lugubris*	variable	Y	Y	Brief stop and head-to-tail contraction, followed by pivoting and moving to cathode	Anisotropy of electrical conductance; alignment with head toward cathode has least resistance

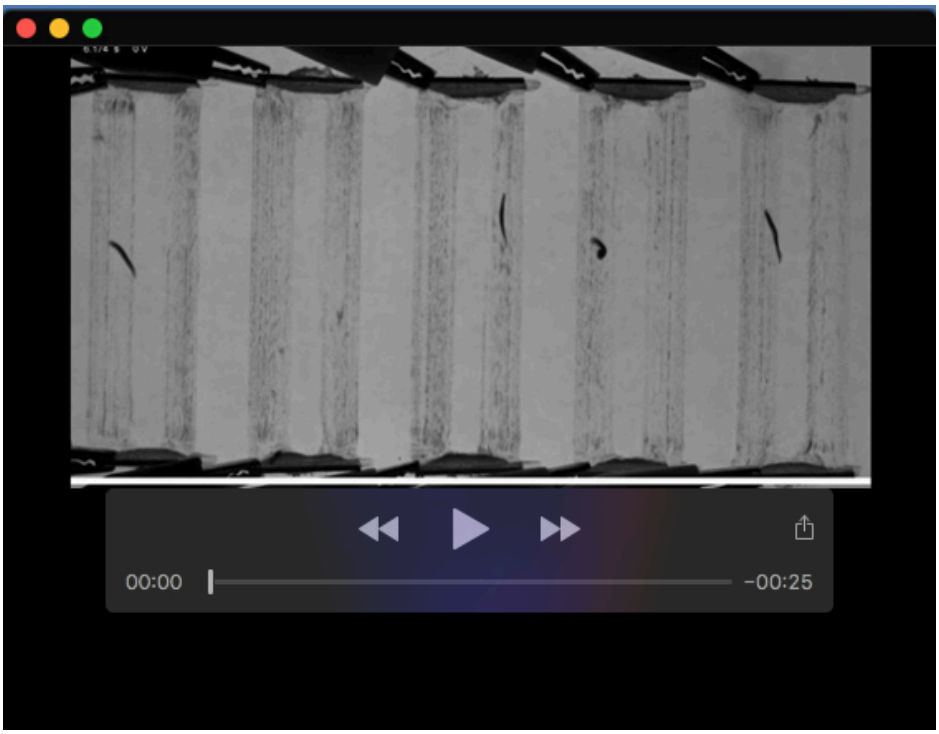

Movie 1. Planarian movement with and without electric field. Planarians move randomly in troughs when no voltage is applied but show directed movement towards the cathode when 2V is applied. Timestamp is in seconds and the white bar represents the location of the cathode. Movie is sped up 4x.

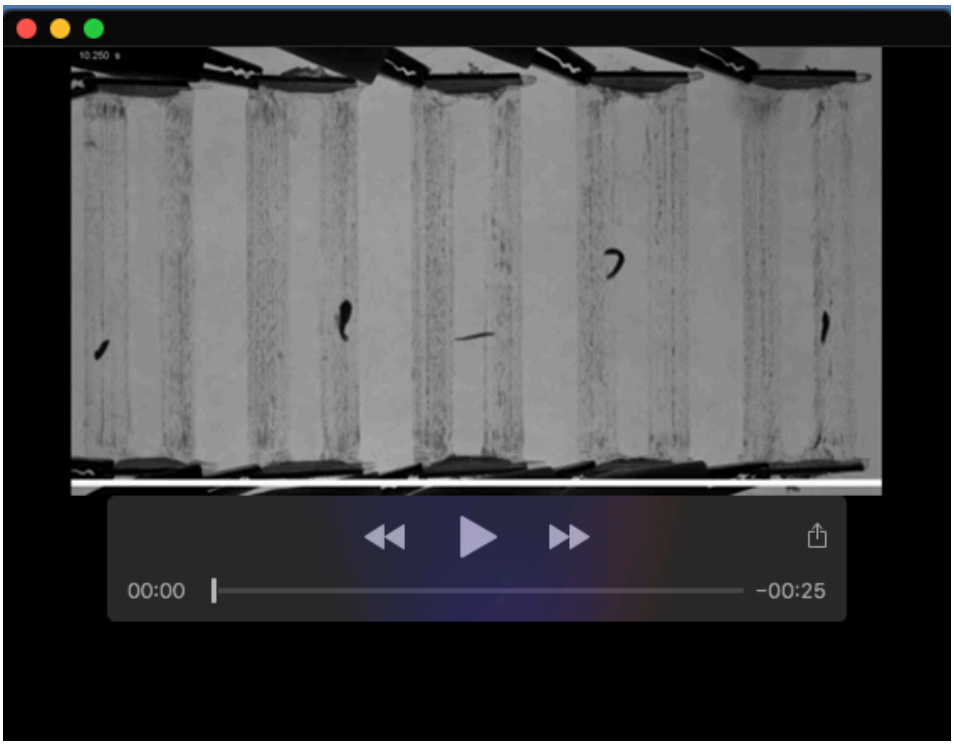

Movie 2. Planarians display muscle-driven locomotion at 4V. Planarians move randomly in troughs when no voltage is applied but show directed movement using muscle-driven locomotion towards the cathode when 2V is applied. Timestamp is in seconds and the white bar represents the location of the cathode. Movie is sped up 4x.

Movie 3. Head removal rescues loss of cathodic electrotaxis in head fragments. The response of head fragments to 2V is shown first, before and after polarity swap, followed by the response to 2V of the same individuals after decapitation and 1 day of healing, before and after polarity swap. The white bar represents the location of the cathode. Movie is sped up 8x.

References

Fries, E.F.B., 1928. Drug action in galvanotropic responses. *Journal of General Physiology*, 11(5), pp.507–513.

Hyman, L.H., 1932. Studies on the Correlation between Metabolic Gradients, Electrical Gradients, and Galvanotaxis. II. Galvanotaxis of the Brown Hydra and Some Non-Fissioning Planarians. *Physiological Zoology*, 5(2), pp.185–190.

Hyman, L.H. & Bellamy, A.W., 1922. Studies on the correlation between metabolic gradients, electrical gradients, and galvanotaxis. *Biological Bulletin*, 43(5), pp.313–347.

Jenkins, M.M., 1967. Aspects of Planarian Biology and Behavior. *Chemistry of Learning*, pp.117–143.

Pearl, R., 1903. The Movements and Reactions of Fresh-water Planarians: A Study in Animal Behaviour; The Quarterly Journal of Microscopical Science. *The Quarterly Journal of Microscopical Science*, 46, pp.509–714.

Robertson, J.A., 1927. Galvanotropic Reactions of Polycelis nigra in Relation to Inherent Electrical Polarity. *Journal of Experimental Biology*, 5(1), pp.66–88.

Viaud, G. & Medioni, J., 1951. Anisotropie d'excitation et variations des seuils de réaction au courant galvanique en fonction de la taille chez Planaria lugubris, O. Sch. *Comptes rendus des seances de la Societe de biologie et de ses filiales*, 145(15–16), pp.1228–31.